



**Politecnico
di Torino**

Politecnico di Torino

Corso di Laurea Magistrale in Ingegneria Biomedica

A.a. 2021/2022

Sessione di Laurea Dicembre 2022

Design of multifunctional and antimicrobial titanium surfaces using polydopamine and antimicrobial peptide

Relatore:

Prof. Gianluca Ciardelli

Candidata:

Teresa Gagliardi

Correlatori:

Prof. Chiara Tonda Turo

Dr. Akhilesh Rai

This work was mainly developed in the Advanced Therapies Group at UC-Biotech (Cantanhede, Portugal), under the supervision of Dr. Akhilesh Rai.



Abstract

Dental defects are very common affecting millions of people around the world. The most common cause of tooth loss is periodontal disease. The formation of bacterial plaque on the tooth surface leads to periodontal diseases. The dental implant is the best option to replace the damaged or the lost tooth; however, poor oral hygiene by the patient causes postoperative inflammation and infections, leading to peri-implantitis diseases. In fact, if peri-implantitis is not prevented, it increases the risk of non-osseointegration by almost 80 times, leading to the subsequent loss of the implant.

In this work, Titanium (Ti) surfaces were functionalized with polydopamine (PDA) followed by conjugation of LL37 peptide, an antimicrobial peptide with regenerative properties. Ti-PDA-LL37 surfaces were active against Gram-positive (*S. aureus* and *E. faecalis*) and Gram-negative (*E. coli*) bacteria upon near-infrared (NIR) light exposure. PDA was chosen for its ability to form coatings on a wide range of different compositions surfaces. Moreover, PDA has photothermal property upon the exposure of NIR laser (808 nm) to increase the temperature in a localized way. Two different coating approaches were used to coat PDA on the Ti surface. FTIR-ATR analysis showed the coating of PDA on Ti surfaces. Contact angle measurement showed that PDA-Ti and Ti-PDA-LL37 surfaces are hydrophilic. Ti-PDA-LL37 surfaces potently killed planktonic form (*S. aureus*, *E. faecalis* and *E. coli*) and biofilm form (*S. aureus* and *E. faecalis*) in the presence of human serum upon the exposure of NIR light for 7.5 min. The obtained results indicate the development of antimicrobial and antibiofilm surfaces, laying the foundations for a new possible strategy to be used in the prevention and treatment of peri-implantitis.

Keywords: Antimicrobial peptide, Polydopamine, NIR light, Antimicrobial activity, Antibiofilm activity, Peri-implantitis, Titanium surface.

Contents

Aim of the Work	1
Introduction	3
1.1 The Dental Background	3
1.1.1 Dental implant complications.....	5
1.1.2 Antimicrobial coatings	6
1.2 Bacteria and biofilm formation	8
1.3 Antimicrobial peptides	9
1.3.1 LL37	12
1.4 Antimicrobial photothermal therapy	13
1.5 Polydopamine	14
Materials and methods	20
2.1 Polydopamine coating	20
2.2 LL37 conjugation	21
2.3 Bacterial Culture	22
2.4 Antimicrobial Activity Tests	23
2.5 Biofilm Tests	24
2.7 Attenuated Total Reflectance – Fourier Transformed Infra-Red spectroscopy 25	
2.9 Quartz Crystal Microbalance with Dissipation monitoring	25
2.10 X-Ray Photoelectron Spectroscopy	26
2.11 Statistical Analysis	26
Results and discussion	28
3.1 Polydopamine coating and characterization	28
3.2 NIR laser measurements	33
3.4 Antimicrobial Activity Tests	34
3.4.1 Determination of the MIC of LL37	34
3.4.2 Antimicrobial effect	36
Bibliography	43

Figures

Figure 1.1: The comparison between the structure of the natural tooth and the two-stage implant one.....	4
Figure 1.2: Different types of dental implants.....	5
Figure 1.3: Steps leading to implant loss caused by peri-implantitis.....	6
Figure 1.4: Biofilm lifecycle.....	8
Figure 1.5: Interactions with bacterial membrane and cell membrane.....	10
Figure 1.6: The two different systems of action of the AMPs.....	11
Figure 1.7: Conversion of tyrosine to dopaquinone.....	14
Figure 1.8: Schematic view of the plaque responsible for the adhesion of mussel.....	16
Figure 1.9: Formation of the polyDOPA network.....	17
Figure 1.10: Color change of the polydopamine solution over time: 6 h, 12 h, 24 h, 48 h, 72 h.....	18
Figure 2.1: Representative schematic diagram to show the preparation of Ti-PDA-LL37 discs.....	21
Figure 2.2: Representative schematic diagram to show the re-culture process.....	22
Figure 2.3: Representative schematic diagram to show the antimicrobial test.....	23
Figure 2.4: Representative schematic diagram to show the antibiofilm test.....	24
Figure 3.1: Different dopamine concentrations.....	28
Figure 3.2: Comparison between PDA coating methods.....	29
Figure 3.3: Presence and stability of the PDA coating.....	30
Figure 3.4: Contact angle.....	30
Figure 3.5: QCM-D monitoring performed on Ti-PDA-LL37 surfaces.....	31
Figure 3.6: XPS analysis.....	33
Figure 3.7: Evaluation of photothermal property of Ti-PDA discs.....	34
Figure 3.8: Determination of the MIC of LL37.....	35

Figure 3.9: Results of antimicrobial tests.....	37
Figure 3.10: Results of biofilm tests.....	38
Figure 3.11: Discs after crystal violet staining.....	39

Abbreviations

AMP antimicrobial peptide

APTT antimicrobial photothermal therapy

ASO Antisense Oligonucleotide

ATR – FTIR Attenuated total reflectance – Fourier transformed infra-red

Bi bismuth

BHI brain heart infusion

Ce cerium

CFU colony forming units

Cl chlorine

Cu copper

F fluorine

I iodine

LB Luria-Bertani

Mefp Mytilus Edulis foot protein

MIC minimum inhibitory concentration

M-PEG Amine methoxypoly(ethylene glycol) amine

N₂ nitrogen

NH₂-PEG-MAL Amine – Poly (ethylene glycol) – Maleimide

NIR near-infrared

OD optical density

PBS phosphate-buffered saline

PDA polydopamine

PEG polyethylene glycol

PTA photothermal agent

QCM-D Quartz crystal microbalance with dissipation

ROS reactive oxygen species

Se selenium

SEM standard error of the mean

TESPSA silane triethoxysilylpropyl succinic anhydride

Ti titanium

TiN titanium nitride

TiO₂ titanium dioxide

Ti-PDA titanium surface coated with polydopamine

Ti-PDA-LL37 titanium surface coated with polydopamine conjugated with LL37

UV ultraviolet

XPS X-Ray Photoelectron Spectroscopy

Zn zinc

Aim of the Work

Globally, antibiotic resistance has been continuously increasing, therefore, it is important to develop new effective strategies against bacterial infections to replace or minimize the usage of antibiotics.

The objective of this work is to develop multifunctional coatings on Ti surfaces having antibacterial properties combined with regenerative capabilities. After placement of dental implants, there is possibility of bacterial infection in gingiva, leading to inflammation and subsequently bone loss, which cause resurgery to replace the implants. Antimicrobial coatings on the implants not only prevent the microbial contaminations but also minimize the infections.

The antibacterial properties are achieved by the coatings of polydopamine, which has photothermal property upon the near-infrared light exposure, leading to a localized temperature increase, and destabilization and damage to the bacterial membrane. However in addition to photothermal therapy, the LL37 peptides are covalently conjugated on the polydopamine-coated surfaces (Ti-PDA-LL37 surfaces) to enhance the antimicrobial efficacy. LL37 peptides has an antimicrobial peptide with osteogenic, angiogenic, wound healing and re-epithelialization properties. The covalently bound LL37 peptides to the surface allow a prolonged action over time and it will therefore be necessary to pay attention to the modality to avoid denaturation.

The other aim of the work is to evaluate the antimicrobial actions of Ti-PDA-LL37 surfaces against Gram-positive and Gram-negative bacteria in the presence of human serum. Moreover, the prevention of biofilm formation by Ti-PDA-LL37 surfaces is also studied in this work.

Chapter 1

Introduction

1.1 The Dental Background

The human oral health is a global problem and among the various disease conditions that can occur in the oral cavity, dental defects are very common health problems, affecting millions of people [1]. According to a study by the National Institute of Dental and Craniofacial Research (2011-2016), 2.2% of adults between 20 and 64 years old are toothless and the remainings have an average of 25.5 teeth [2].

Among the various reasons such as dental trauma and caries that lead to tooth loss, the most common is periodontal disease. The periodontium consists of alveolar bone, gingiva, periodontal ligament and root cement. Periodontitis is an inflammatory disease of the periodontium, which leads to the formation of periodontal pockets, tooth mobility and resorption of the alveolar bone. This in the most advanced stages, leading to the loss of the tooth [3], [4]. It is important to consider that there are about 700 species of different microbes including bacteria, viruses and fungi in the oral cavity. Some of these are useful in order to maintain health inside the mouth, while others can lead to tooth loss and gum disease [5]. The most common risk factor for periodontium disease is the formation of bacterial plaque on the tooth surface.

The presence of tartar, which is the deposits made up of limestone and desquamated epithelial cells of the oral mucosa, on the teeth promote the formation of bacterial plaque. Smoking even without causing periodontium disease can lead to gingival recession and bone resorption. In case of development of the disease caused by smoking, the more the subject smokes, the more the chances of contracting the disease in a severe form will be high.

Sensitivity to the periodontal disease may increase in the presence of systemic diseases such as insulin dependent diabetes, Down syndrome, rheumatoid arthritis and HIV infection, but

also if the following drugs are used: steroids, cyclosporins, oral contraceptives, calcium channel blockers, and others [3, 6].

In the case of dental loss or a dental disease in which the best prognosis for the patient would be the removal of the tooth rather than trying to save it, dental implants must be introduced [7].

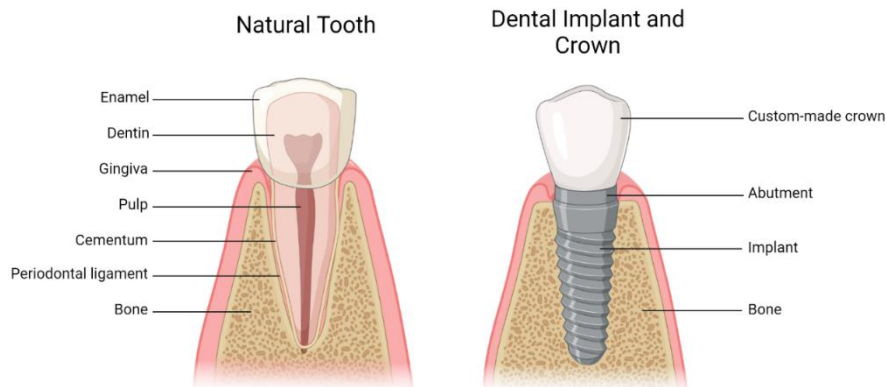


Figure 1.1: The comparison between the structure of the natural tooth and the two-stage implant one[8].

Bone implants in the dental sector can be endosseous, so they cover the inside of the bone without crossing it completely. In this category there are at least two types: the blade-shaped ones and the cylindrical or screw ones, which belong to the same category but can be distinguished by the shape of the implant, which in one case has no thread and in the other is a screw. Endosseous blade implants are those of the older generation (1960s) and have met with some success but are still quite invasive as they intervene on an important amount of bone. Furthermore, especially the former, they were not always made with materials and morphologies capable of guarantee good osseointegration. Several materials such as titanium (Ti), ceramics, zirconium and alumina have been used to make dental implants.

To promote osseointegration, different strategies can be adopted including: simple mechanical processing which leaves small grooves on which the bone can grow, the surface can be sandblasted using alumina, titanium dioxide, silica or even hydroxyapatite, it can be used plasma spray with chemical treatments [9], [10].

Instead, implants that go through the entire thickness of the bone until they come out and possibly be fixed with plates are called transosseous implants. This is when the endosseous implant, also called osseointegrated implant, cannot be used because the bone is too thin, and

then a bit more invasive implants are used. The final purpose is to bring out from the surface of the bone some pins on which to mount the external part.

Implants that do not cross the bone but rest on it are called subperiosteal implants. They are used when the thickness of the mandibular bone is too thin and small, that is, when the blade or screw implant does not have enough bone on which to anchor. These also have the purpose of having abutments on which, for example, an entire arch can be hooked.

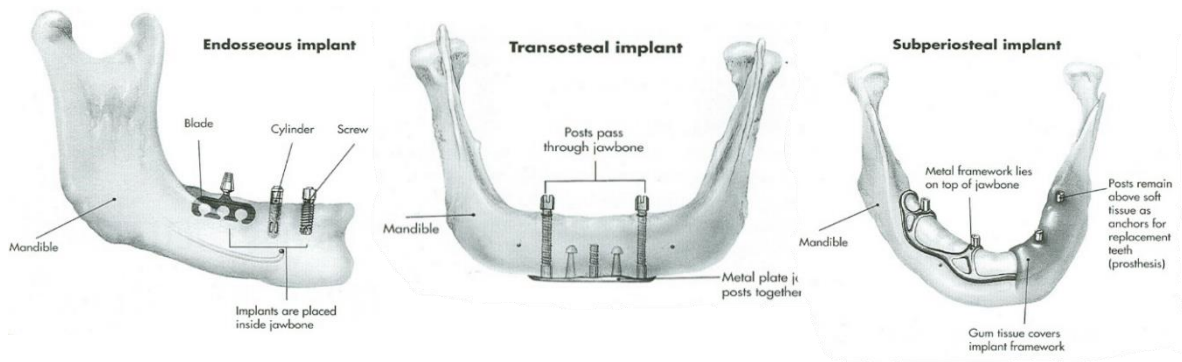


Figure 1.2: Different types of dental implants [11].

1.1.1 Dental implant complications

After the procedure to fix the dental implant, inflammation, infections, mechanical problems and other complications such as fracture of the jaw, bleeding, devitalization of the teeth around the implant can occur, which compromise its success. Mechanical problems can be caused by the inadequate presence of the surrounding bone, the absence of posterior teeth that can support the implant, and also mistakes made during the implantation phase, such as the incorrect angle or position of dental implant [12].

After implantation, the patient must have proper oral hygiene, this is very important to avoid postoperative inflammation and infections. In the presence of infection, the area can be red, swollen and painful, this if not discovered and treated correctly can lead to implant failure due to bone resorption. Furthermore, infections can be triggered by an imbalance of the oral microenvironment caused by antibiotics administered topically and for a short period of time after surgery. These types of infections are resistant to antibiotics and thus lead to subsequent

removal of the implant. Postoperative infections are estimated to increase the risk of non-osseointegration by nearly 80 times [12], [13].

The pathological condition the patient can develop after dental implantation, characterized by inflammation of the connective tissues surrounding the implant and progressive bone resorption, is known as peri-implantitis [14], [15]. It is important to point out that there are two types of peri-implant diseases: peri-implant mucositis and peri-implantitis. The first can also lead to the development of the second. The substantial difference between the two conditions is that peri-implant mucositis does not affect the bone that supports the implant but only the soft tissues that surround it [14], [16]. Insufficient oral hygiene, inadequate care of the implant area after the operation but also a history of chronic periodontitis are factors that lead to greatly increase the risk of developing the disease.

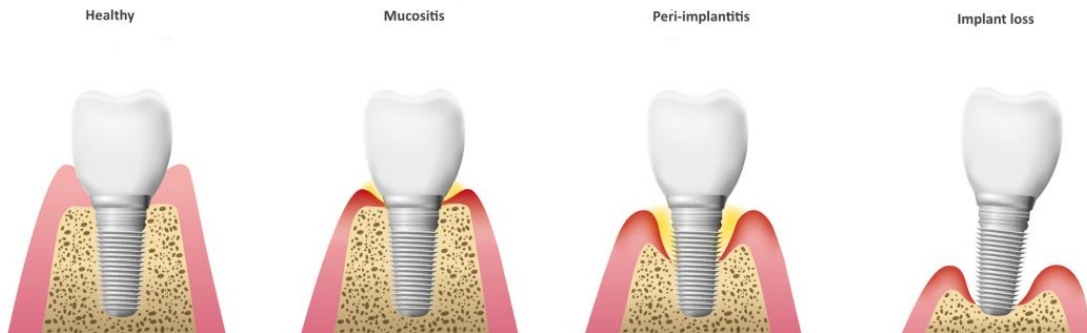


Figure 1.3: Steps leading to implant loss caused by peri-implantitis [17].

1.1.2 Antimicrobial coatings

To ensure an antimicrobial and antibiofilm effect, coatings of various materials are used on the implant. Polyethylene glycol (PEG) is often used among polymer coatings on titanium (Ti) surfaces. PEG has antifouling properties, which is useful against bacteria but hinder osseointegration in the bone tissue [18]. Totarol is a natural substance with an antibacterial effect. Studies have been carried out on its effectiveness on Ti surfaces. It was seen that after 12 days of treatment, the bactericidal properties had decreased as opposed to the bacteriostatic ones. Therefore, Totarol is considered to be a promising agent in the prevention of infections in case of implantation [19]. Biosurfactants have been used against bacteria and

biofilm formation. Experiments were carried out on Ti surfaces, showing good results in terms of antifouling properties thanks to their amphiphilic structure and not being cytotoxic [20]. On the other hand, bactericidal materials such as antimicrobial peptides (AMPs) have been considered to be alternative to antibiotics and have multifunctional properties [21]. AMPs can be used in place of antibacterial materials such as silver having both antibacterial and osseointegration capabilities [22]. Moreover, ions from some elements can also have antibacterial properties [23]. Among them are copper (Cu), chlorine (Cl), zinc (Zn), fluorine (F), iodine (I), cerium (Ce), selenium (Se) and bismuth (Bi) [24].

Titanium dioxide (TiO₂), also known as titania, is used as an antibacterial coating. Thanks to the exposure of titania to strong UV light, reactive oxygen species (ROS) are produced which are able to eliminate many microorganisms including bacteria [25], [26].

Metal nanoparticles obtained from silver, gold but also from zinc and copper are used for their antimicrobial properties. Those normally used are silver nanoparticles, which are coated on a titanium surface, increase its bacteriostatic and bactericidal properties. Their antimicrobial mechanism is not fully understood, however the released silver ions from the surface produce ROS inside the bacteria, leading to bacterial death [27].

Coatings loaded with antibiotics have also been developed on Ti surfaces. However, there are certain limitations with antibiotic coatings. For example, the rate of release was too fast to provide sufficient coverage for the development of infections during the postoperative period [28]. Some concerns have been developed regarding toxicity and the development of antibiotic resistance [22]. In fact, the antibiotic burst release revealed how it can cause toxicity in nearby tissues. Another fact to consider is that antibiotic resistance can be caused by drug release below the minimum inhibitory concentration level (MIC) [29]. Furthermore, many of the studies conducted so far have not been done in conditions that reproduce the oral cavity [30].

Usually explored to bind various molecules such as proteins, peptides and polymers to titanium surfaces, silane has also been shown to have bactericidal properties. For example, silane triethoxysilylpropyl succinic anhydride (TESPSA) has demonstrated osteoinductive but also antibacterial capacity for a prolonged period [31]. A coating that would need other studies due to uncertain results is that of nitride [32]. In fact, titanium nitride (TiN) is chemically stable, manages to remain biocompatible even at high temperatures and is characterized by good resistance to corrosion [25]. Chlorhexidine also proved effective in a short time in the field of bacterial infections [33].

In case of new strategies, the Antisense Oligonucleotides (ASOs) have generated a lot of interests in scientific communities. They are fragments of nucleic acids that have the ability to counter biological processes in bacteria [34]. Their targets can be mRNA and rRNA that code for essential genes but also interfere with genes that are involved in biofilm formation or adhering to a surface [35], [36].

Even in the case of bacteriophages (phages) there is a need for more evidence in favor of their efficacy. Bacteriophages are viruses capable of infecting bacteria and leading them to lysis thanks to the insertion of their genetic material within the bacterial one [37], [38]. There are good premises on their use as they would be able to infect only certain strains of bacteria, allowing those that are part of the healthy environment inside the oral cavity to remain undisturbed[39]. Finally, there have recently been studies on the effect of photodynamic and photothermal therapy combined with antimicrobial coatings [40]–[42].

1.2 Bacteria and biofilm formation

The bacteria present in the oral cavity form biofilm on the surfaces they come into contact with. The bacteria may live on their own, but it has been observed that most bacteria tend to form these communities called biofilms. Its formation takes place in steps. Initially the bacteria settle and begin to be adsorbed, not all of them because a part will be desorbed in the external environment. When they begin to adhere more stably, they initiate to produce matrix, thus starting to form biofilms [43].

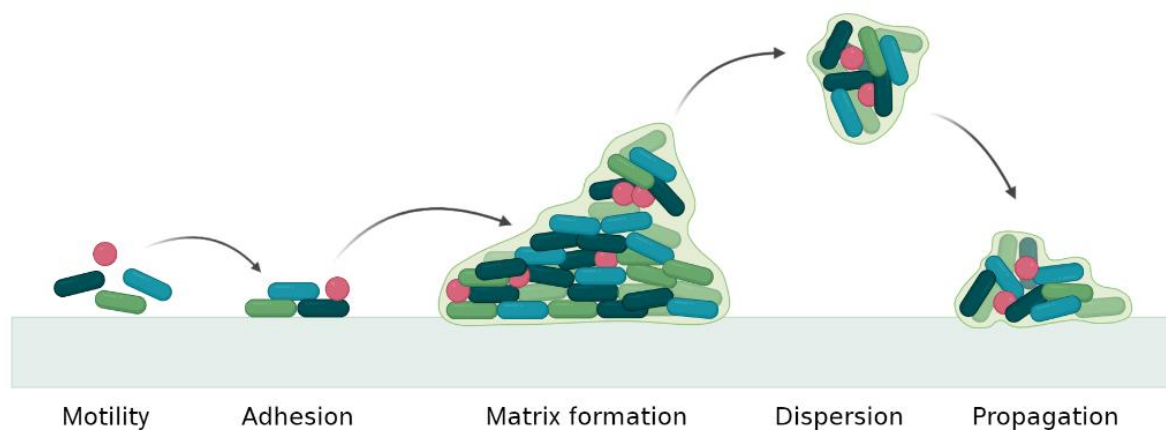


Figure 1.4: Biofilm lifecycle [8].

The matrix produced is mainly made up of secreted polysaccharides and contains the various populations of bacteria. Furthermore, within the biofilm the diffusion of nutrients is slowed down due to the very dense matrix. Bacteria in biofilm communicate with each other even if far away due to quorum sensing, communication occurs through the production of substances that reach other bacteria through the biofilm [43], [44].

By developing the biofilm vertically, the bacteria have a better chance of reaching nutrients but also lend themselves to the detachment of infectious emboli. When an embolus detaches, for example, in the case of an in vivo device it can carry the infection to other parts of the body.

Bacteria in planktonic form are easily accessible by macrophages, drugs and antibiotics, therefore, they are very vulnerable. When these are able to colonize the surface and then organize themselves within the biofilm, drugs, antibodies and macrophages cannot reach them. The macrophages remain in the infected area, they try to destroy the bacterial biofilm and produce substances such as degradative enzymes which, however, have no effect on the biofilm but on the nearby healthy tissues which can suffer. This can generate inflammation that persists leading to chronic inflammation. The bacteria, on the other hand, remain viable and are not affected by the action of macrophages or antibiotics.

There is therefore a need to use surfaces that minimize adhesion and bacterial proliferation. These can be divided into antibiofouling surfaces, which bacteria cannot adhere to, and antimicrobial surfaces. The second type of surfaces can be divided into bactericidal, which cause the death of bacteria, and bacteriostatic, which inhibit their growth [44], [45].

1.3 Antimicrobial peptides

Nature offers us bactericidal substances and an example is antimicrobial peptides (AMPs). They are effective not only against bacteria but also against fungi and viruses. Furthermore, some AMPs have tissue regeneration, bone regeneration and immunomodulation properties [46]. One of the most important characteristics of AMPs is the low ability to develop antimicrobial resistance due to their low affinity targets [47]. They can be engineered to improve such as bioactivity and cytotoxicity [48], [49].

AMPs consist of a sequence of amino acids linked together by peptide bonds. In particular, they are formed by less than 100 amino acids having a total charge of +2 up to +9, due to the presence of positively charged amino acids such as lysine and arginine [50], [51]. The sequence of amino acids present is amphiphilic, therefore hydrophilic and other hydrophobic parts are present [52]. AMPs are produced by various mammals, plants, fish, insects and microorganisms [53]–[57]. To date, more than 2600 AMPs have been documented, usually they are cationic but there are also non-cationic ones [58].

There is an action of the AMP against the cell membrane, but it is weak and is linked to the amphiphilic characteristic of the peptide. The bacterial membrane is characterized by a slight negative charge so there is a strong electrostatic interaction with cationic AMPs that favors a sort of specialization of the AMPs towards the bacteria themselves [52].

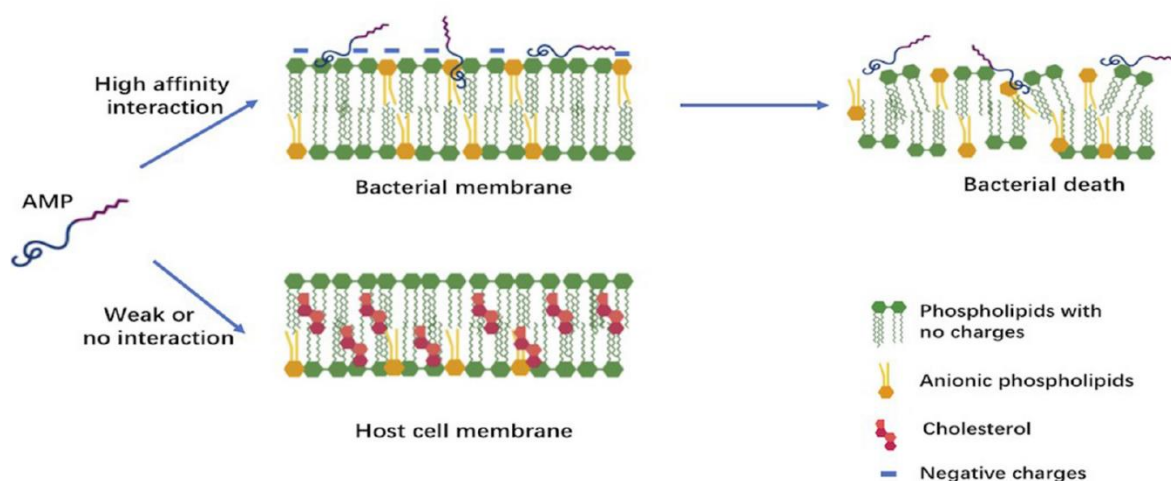


Figure 1.5: Interactions with bacterial membrane and cell membrane. In the presence of a bacterial membrane there are electrostatic and hydrophobic interactions with cationic AMPs. In the case of cells, the interactions present are only the hydrophobic ones [52].

The mechanisms of action of peptides can be of two types. The first is the surface interaction of the AMPs, therefore with the membrane of the bacteria, in this case we can have various models that describe the situation.

There is the barrel stave model in which a not excessive amount of AMPs come into contact with the bacterial membrane, causing a depolarization of the membrane with the formation of pores, leading to the cell death. When the amount of peptide is very high, on the other hand, it can be said that the carpet model is valid. In this case the effect could be the

destruction of the bacterial membrane or the depolarization of this which would again lead to the formation of pores, in this case called toroidal model pores, with consequent bacterial death (Figure 1.6A) [51].

However, some AMPs do not act on the membrane but act differently, usually they are non-cationic peptides. In this case, the peptide is internalized by the bacteria in vesicles and then released into the cytoplasm, acting internally, altering its behavior and ultimately leading to bacterial death (Figure 1.6B) [52].

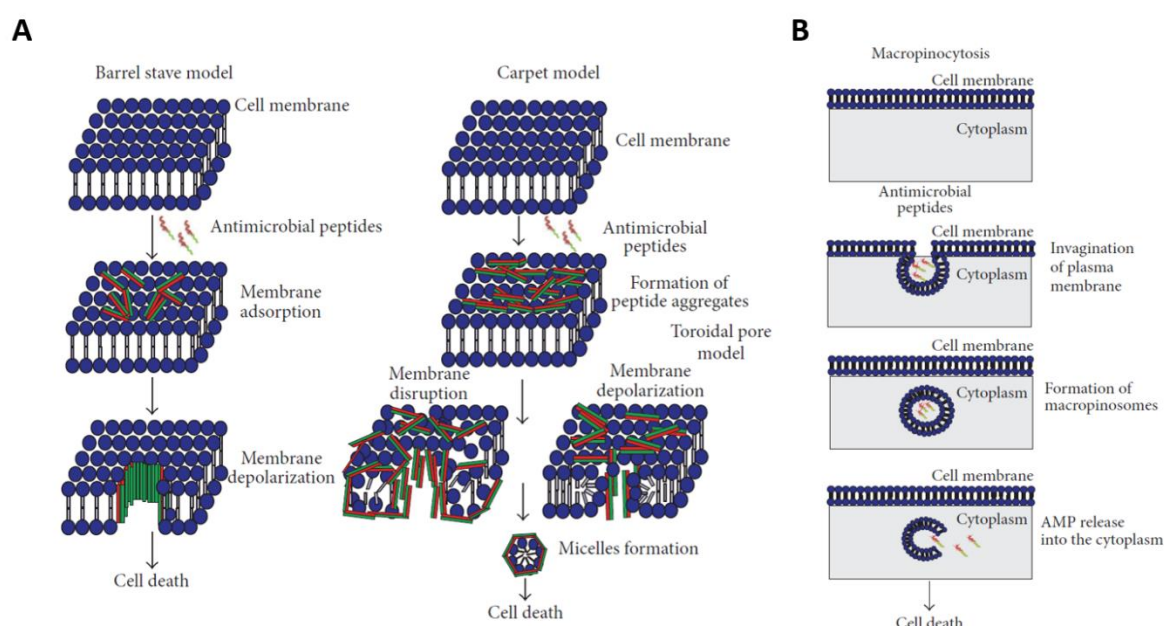


Figure 1.6: The two different systems of action of the AMPs. A) Barrel stave model, carpet model and Toroidal pore model, independent ATP mechanisms. B) Macropinocytosis, dependent ATP mechanism [50].

AMPs can be effective against both Gram-positive and Gram-negative bacteria. In addition, they kill bacteria very quickly, which is important because the bacteria cannot develop resistance to antimicrobial peptides in this way which they do to antibiotics. In fact, antibiotics have a more specific mechanism of operation, so it is easier for bacteria to develop resistance. On the other hand, peptides have a much wider action: they destroy the membrane, act from inside the bacterium, have anti-inflammatory power, also have anticancer effects and some antiviral effects [59]–[63].

However, there are also negative aspects including toxicity. As a matter of fact, AMPs are more specific for bacteria but can also act on tissue cells. In order to test the toxicity of AMPs, the hemolysis tests are performed to test their effect on red blood cells, as they are extremely

sensitive to peptides [64]. AMPs are also easily degradable by enzymes. If administered systemically they can undergo rapid degradation reducing the time of efficacy [47], [65]. AMPs are sensitive to process conditions, i.e. pH, can easily denature and therefore no longer be effective [66], [67]. Some allergies can be induced by AMPs if they are used for a long time [65]. Finally, they have costs that are quite high as regards their synthesis[52].

AMPs can be used to functionalize surfaces and therefore can be bonded to the surface in a non-covalent or covalent way [68], [69]. An example could be linking it covalently to the surface, keeping it active and being careful not to denature it. Another example, in case of non-covalent functionalization of the surface, could involve the use of a cationic peptide and through the layer-by-layer technique to trap the AMP inside the layers at least initially. When the layers begin to flake the peptide is released and activated [70]. It is possible to create gels that trap the peptide inside and subsequently release it gradually over time, or gels in which the peptide is covalently linked, thus obtaining a gel that has a continuous bactericidal power over time [71], [72].

There are also new solutions that rely on AMPs to generate different materials. They could be polymers, materials that mimic antibacterial peptides due to their amphiphilicity, so one could think of using them to produce objects and devices that are inherently antibacterial [73].

1.3.1 LL37

As mentioned above, AMPs are not only capable of killing bacteria, but they can also have other properties. For example, cathelicidins in addition to being antibacterial peptides are able to modulate and stimulate the immune response, have the ability to promote osteogenic differentiation, the ability to encourage wound healing, induce re-epithelialization and also possess angiogenic properties [74]. LL37 is the most studied peptide belonging to the cathelicidins group and the only one in humans [52].

In 1995, hCAP18, a member protein of cathelicidins, was discovered in humans. LL37 was the peptide positioned at the C-terminal end of the hCAP18 protein [75]. This AMP has 37 amino acids and its sequence begins with two leucines. It is a cationic peptide which, coming into contact with the bacterial membrane, positions itself in such a way as to cause the formation of transmembrane pores and lead to bacterial death [74], [76]. LL37 is effective

against Gram-positive and Gram-negative bacteria, but also against fungi and has antiviral properties [77], [78].

As for the biofilm, studies have been conducted regarding both the efficacy against already formed biofilms and the efficacy that this peptide has in preventing its formation. It has been seen that in the first case the presence of the peptide led to a downregulation of the genes that are usually controlled by quorum sensing with a consequent decrease in the ability of the bacteria to adhere to the surface and in the cohesion between them. It has also shown a promise against biofilm formation. In fact, non-human cathelicidins have also been tested and no efficacy has been found [79], [80]. In diseases and pathologies such as chronic wounds, cancer, sepsis and many others, the use of LL37 could be very useful.

Finally, it has been seen through some studies that the use of the immobilized peptide on surfaces is preferable as it is more stable and effective than its soluble version. In fact, even if it is not yet clear why the soluble peptide appears to have lower healing and pro-angiogenic capabilities [81].

1.4 Antimicrobial photothermal therapy

Antimicrobial photothermal therapy (APTT) appears to be a valid and promising strategy in the dental field. Due to inappropriate prescriptions, prolonged treatment cycle and the usage of antibiotics in feed for livestock for preventive purposes, several strains of bacteria resistant to antibiotics have developed. Vancomycin-resistant *Enterococcus faecium*, Methicillin-resistant *Staphylococcus aureus* and Multidrug-resistant *Acinetobacter baumannii* are antibiotic-resistant bacteria [82].

APTT is a physical sterilization due to the presence of photothermal agents (PTAs) combined with the light irradiation. It causes a localized temperature increase leading to the death of the bacteria. Through the hyperthermia caused by APTT, various effects such as evaporation of the cellular fluid, enzymatic and protein denaturation, rupture of the membrane and cell cavitation could occur [83], [84]. Photothermic therapy has been shown to be effective against a wide range of bacteria and capable of eliminating bacteria in solution to sterilize its contents. Furthermore, it is not possible for bacteria treated with this therapy to develop resistance [85], [86]. Several PTAs can be used for this purpose. For example, as nanomaterials gold nanoparticles, nanorods, nanoshells or nanostars [87]–[90]. Graphene is

also a possible PTA and can be found as graphene oxide or reduced graphene oxide [91], [92]. MoS₂, MnO₂, Bi₂S₃, polydopamine and polyaniline are other possible PTAs [93]–[97]. An important feature of PTAs is the ability to transform part of the absorbed light into thermal energy to raise the temperature.

In particular, more tests on the biocompatibility of some formulations, PTAs capable of converting a large amount of absorbed light thus having a high conversion efficiency, also combining other capacities to the photothermic one as antithrombus properties would be interesting to develop [83]. The method by which the PTA is stabilized on the surface is also important. We can use a physical methods such as electrostatic interactions, hydrogen bonding, covalent bonds to load PTA on the surface [98], [99]. In fact, to eliminate the bacteria alone it can exceed the irradiance limit, i.e. 0.32 W/cm² following the American National Standard Institute Laser Safety Standards [100]. Another possibility is that the temperature needed for the purpose can damage surrounding tissues [101]. It is therefore useful to combine this antibacterial strategy with others, such as silver nanoparticles and nanoplates [88], [102].

1.5 Polydopamine

3, 4 - dihydroxyphenylalanine (DOPA) is an amino acid abundant in mussel proteins. In 1981 it was studied by Waite and Tanzer, they discovered that it appears to be the key component for the adhesion of the mollusc in an aqueous environment, an obstacle instead for synthetic glues [103], [104].

DOPA is obtained through the oxidation of tyrosine which in turn tends to partially oxidize in the marine environment and become DOPAquinone. Oxidation is due to the marine pH which is slightly alkaline (8.5), in these conditions DOPA and DOPAquinone are in equilibrium [105], [106].

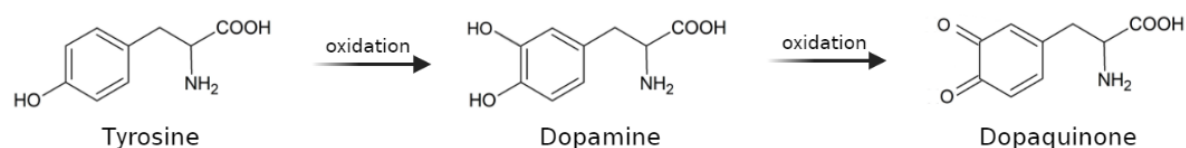


Figure 1.7: Conversion of tyrosine to dopaquinone[8].

The mussel adheres to the substrate due to filaments ending in plates, about a few mm large. These filaments can be up to several centimeters long and are generally arranged radially. This is a way for the mollusk to have a stable adhesion in different directions against the inevitable shear stresses in the marine environment. These filaments with which the animal adheres are protein filaments, precisely formed by 25-30 proteins. Externally, along the outer surface of the filament and also at the plaque are a series of polyphenolic proteins. Internally, in the core of the filament, there are collagen proteins of different types, arranged in a gradient so that the filament is more extensible in the parts closest to the body of the mollusk and less extensible and stiffer outside [107], [108].

Through special glands the mollusk secretes liquid protein precursors, these are extruded towards the outside. As soon as they are in contact with the sea water, which has a slightly alkaline pH (8.5), the filament stabilizes and reticulates on its surface, therefore a rigid cuticle is formed, which stabilizes its shape to avoid deformation of the filament [107].

Furthermore, the filaments of the byssus through the stem are in contact with the internal musculature, with the retractor muscles of the byssus, therefore the animal has its own muscles through which it is able to contract the filaments and therefore to modulate the adhesion tension. The other muscles present, the adductors, have nothing to do with adhesion but only serve to open and close the shell [107], [109].

Looking at the section of a byssus filament, the contact with the retractor muscles at the proximal end is noted, then this thin filament departs which internally presents a series of collagen-based proteins and externally these polyphenolic proteins that form a reticulated cuticle. These polyphenolic proteins are called "Mytilus Edulis foot protein" (Mefp). Approaching the plaque the shape changes, there are no more collagen proteins but only polyphenolic proteins of various types, it is noted that the Mefp types 3 and 5 are those in direct contact with the substrate and therefore determine the adhesion [109]. The composition of these proteins has been studied and it has been discovered that they are rich in an amino acid, that is DOPA [110].

It can also be noted that a high amount of DOPA is also present in the protein Mefp-1 that surrounds the filament. This means that on the surface of the filament there is a part of the DOPA groups that have been converted into dopaquinone, these functionalities are reactive, they can react with other molecules with thiol or amino groups and it is possible to find these groups on the proteins themselves. So as soon as the marine pH leads to the formation of

dopaquinone, they begin to react with functionalities present in the same protein and a cross-linked cuticle is formed [107].

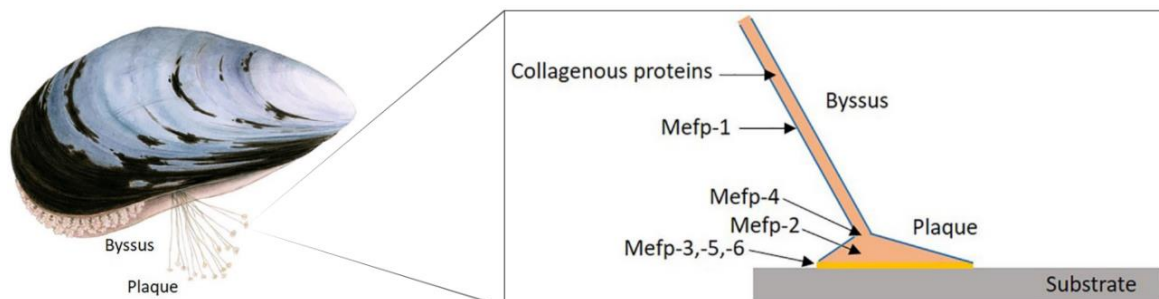


Figure 1.8: Schematic view of the plaque responsible for the adhesion of mussel [8], [107].

The abundance of catechol groups in DOPA and quinone in DOPAquinone explains how the mussel is able to adhere due to the former to surfaces of inorganic nature and through the latter to organic surfaces. In particular, with inorganic surfaces it is able to form hydrogen bonds with hydrophilic surfaces and strong metal complexes with metal ions, while organic surfaces containing primary amino or thiol groups are reactive with the quinone groups present forming covalent bonds.

Oxidizing DOPA leads to the formation of cross-linked films having catechol and quinone groups that can be exploited for subsequent functionalization steps [103]. In the presence of basic pH, the catechol groups which oxidize into quinone groups are very reactive and can also undergo various secondary reactions which lead to the formation of brownish pigments. Among the side reactions can be named reactions with amino groups and reactions with thiol groups. In particular, quinone groups can react with amino groups via Michael addition or Schiff base reaction (Figure 1.9A). It has been seen that normally in the presence of aromatic amines the Michael type addition is favored, on the contrary in the case of aliphatic amines the Schiff base reaction is favored [104], [111].

As regards possible parameters that influence the Michael addition, pH is certainly one of them. An increase in pH leads to a higher reaction rate. A lower reaction rate, on the other hand, can be caused by a substitute in the aromatic ring of the catechol, for example as in the case of 4-methylcatechol in the presence of which a lower reactivity is recorded compared to

unsubstituted catechol [112]. The basicity of the amine is another factor affecting the reaction rate, this will be greater with more basic amines [113].

The pH and the length of the chain containing the primary amine are the parameters that influence Schiff base reactions. More precisely a decrease in the basicity of the primary amine is caused in the presence of a longer chain, this will lead to the possibility of the reaction to take place even at lower pH [104].

If, on the other hand, thiol groups are present, they will react with polyDOPA through a Michael addition reaction (Figure 1.9B) [111]. A higher oxidation rate of the catechols leads to a higher efficiency of the reaction. Furthermore, higher reactivity is obtained in the presence of primary thiols with lower steric hindrance [114], [115].

However, it should be borne in mind that only possible explanations on the exact structure of the polyDOPA have been presented [110].

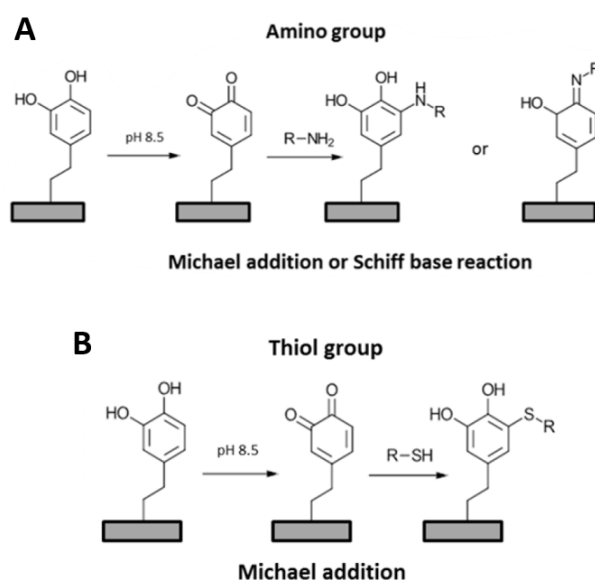


Figure 1.9: Formation of the polyDOPA network. (A) Formation of the covalent bond by Michael addition and Schiff base reaction in the presence of amino groups. (B) Formation of the covalent bond by Michael addition in the presence of thiol groups [111].

The amino acid DOPA can be artificially produced, and it is possible to obtain adhesive gels or intermediate surface functionalizations to subsequently adhere on peptides and proteins [103]. Another interesting feature of polyDOPA is that regardless of the material and therefore the chemistry of the coated surface, the coating will make it hydrophilic [116].

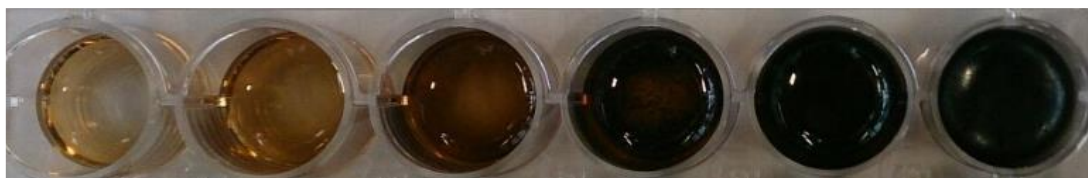


Figure 1.10: Color change of the polydopamine solution over time: 6 h, 12 h, 24 h, 48 h, 72 h. The brownish color reached by the solution is the one that can also be seen on the surface immersed in it [117].

There are five parameters to be optimized for the formation of a polydopamine coating. As the hours in solution increase, the thickness of the film formed on the surface increases, reaching a plateau at 24 h [103], [118]. Increasing the concentration of dopamine in solution will result in greater efficiency [119]. A higher coating efficiency can also be obtained by increasing the temperature [120]. pH ranges have been identified with which different results are obtained. Specifically, at $\text{pH} \leq 4.5$ there will be a limited coating, with pH 7 the efficiency level will be moderate, pH 8.5 is the best, as opposed to $\text{pH} \geq 11$ in which unstable coatings are obtained [119], [121], [122]. Finally, higher oxidation levels will result in greater coating efficiency [123]. However, it must be emphasized that the fundamental parameter of all remains the pH [116].

Chapter 2

Materials and methods

2.1 Polydopamine coating

Ti discs with a diameter of 1.3 cm were used to do the PDA coating and subsequently functionalization of LL37 peptides.

To do the PDA coating on the surface, the first step is cleaning the discs in 5M NaOH (Emprove® Essential, Germany) solution for 30 min at 60 °C. After washing the discs in Milli-Q water and drying them with nitrogen (N₂) gas, the dopamine solution is prepared. For this purpose, dopamine hydrochloride (Sigma-Aldrich, Germany) combined with 10 mM Tris buffer (pH 8.5, Acros Organics, Germany) was used. Once 260 mM dopamine solution is obtained, the discs are placed in a 24-well plate (VWR International, USA) and 1 mL of solution is added to each Ti discs and left 24-well plate uncovered in the dark for 15 h. Finally, the discs are washed with Milli-Q water and dried with N₂ gas. The concentration of 260 mM was chosen after testing with solutions at different dopamine concentrations. Once the coating on the surface was obtained, the absorbance was measured using a spectrophotometer-microplate reader (SYNERGY H1, BioTek Instruments, USA).

A different method has also been explored to do the PDA coating in lesser time, called ultrafast coating. In fact, 0.5 mL of 260 mM dopamine solution in Milli-Q water is placed in the well with 0.5 mL of a solution formed by 6 mM NaOH, 100 mM Tris buffer and 160 mM KMnO₄ (Honeywell™ Fluka™, Germany). Then the plates are left uncovered in the dark for 1 h, before the discs are washed with Milli-Q water and dried with N₂ gas.

PDA coated discs were loaded with CuCl₂ (Sigma-Aldrich, UK) as the second step. Ti-PDAs were placed in a 24-well plate and 1 mL of 20 mM CuCl₂ solution was placed in each well. The plate was then placed on the shaker at 150 rpm for 3 hours.

2.2 LL37 conjugation

Place the Ti-PDA discs in a new 24-well plate and add 1 mL of 100 $\mu\text{g/ml}$ M-PEG Amine solution (Methoxypoly(ethylene glycol) amine, MW 1k, Creative PEGWorks, USA) in 10 mM Tris buffer to each well. Put the plate on a shaker for 1 h at 150 rpm. Then rinse in 10 mM Tris. Thanks to the ability of the PDA to react with amino or thiol groups through Schiff base and Michael addition reaction (Figure 1.9), the M-PEG Amine will be able to bind to the Ti-PDA surface.

Again, place the discs in new wells by adding 1 mL to each of 1000 $\mu\text{g/ml}$ NH_2 -PEG-MAL (Amine – Poly (ethylene glycol) – Maleimide, MW 1k, Creative PEGWorks, USA) in 10mM Tris buffer. Put the plate on the shaker for 1.5 h at 150 rpm. Wash in 10 mM Tris buffer. Also in this case NH_2 -PEG-MAL will bind to the surface due to the ability of the PDA to react with amino or thiol groups (Figure 2.1).

Finally, the solution with LL37 1000 $\mu\text{g/ml}$ peptide (peptide having a cysteine residue at C-terminus, LLGDFFRKSKEKIGKEFKRIVQRIKDFLRNLPRTESC-NH₂, purity of 96%, Caslo Laboratory, Denmark) dissolved in phosphate-buffered saline (PBS) was added in PDA-Ti discs in 24 well plate. The plate is placed on the shaker for 2 h at 150 rpm, then the plate is kept overnight at 4 °C. The next day the discs are washed in PBS and dried with nitrogen gas. The peptide will bind covalently due to the presence of the thiol group at the NH_2 -PEG-MAL linker through the thiol-maleimide chemistry (Figure 2.1).

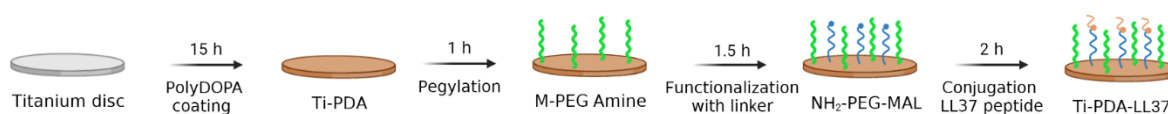


Figure 2.1: Representative schematic diagram to show the preparation of Ti-PDA-LL37 discs.

The surface bound peptide was quantified by measuring the absorbance considering 258 nm as the characteristic peak of LL37, due to the presence of phenylalanine residues. The absorbance of the original peptide solution was measured, and the measurement was repeated with the supernatant after conjugation of the peptide on the surface. The amount of LL37 conjugated on Ti-PDA discs was quantified by subtracting amount of added peptide to amount in supernatant. The Beer-Lambert formula was used to quantify the amount of peptide.

2.3 Bacterial Culture

Two different media were used for different strains of bacteria, specifically Luria-Bertani (LB) media and brain heart infusion (BHI) media. To prepare 1L of LB media, the following substances were weighed: 10 g of peptone bacteriological (Liofilmchem S.r.l., Italy), 5 g of yeast extract (Liofilmchem S.r.l., Italy), 5 g of sodium chloride (ITW Reagents) and 1 L of Milli-Q water. LB agar was obtained in the same way but by adding 17 g of agar (Liofilmchem S.r.l., Italy). For BHI media, 37 g of BHI broth (Liofilmchem S.r.l., Italy) were combined with 1 L of Milli-Q water. The BHI agar was prepared by weighing 47 g of BHI agar (Liofilmchem S.r.l., Italy) and adding 1 L of Milli-Q water. All solutions were autoclaved. LB agar and BHI agar were poured into petri dishes inside a biological hood in order to obtain LB and BHI agar plates.

Experiments using Gram-positive and Gram-negative bacteria were conducted to evaluate the antibacterial activity of Ti-PDA-LL37. Among the Gram-positive, *Staphylococcus aureus* (*S. aureus*, DSM 799) and *Enterococcus faecalis* (*E. faecalis*, ATCC 19433) were used, as Gram-negative instead *Escherichia Coli* (*E. coli*, ATCC 25922) were used. Bacteria were stored at -80 °C. Subsequently, using a spreader 20 µL of bacterial solution were cultured in LB agar (*E. coli* and *S. aureus*) or BHI agar (*E. faecalis*) plates. After 24 h in incubator at 37 °C, bacterial colonies grow on LB or BHI agar petri dishes.

In order to keep the bacteria viable, re-culture was carried out (Figure 2.2). Therefore, a bacterial colony was taken and, with the aid of a loop, it was re-cultured in a new agar plate then placed in an incubator at 37 °C. Re-culture was repeated every 48 h.

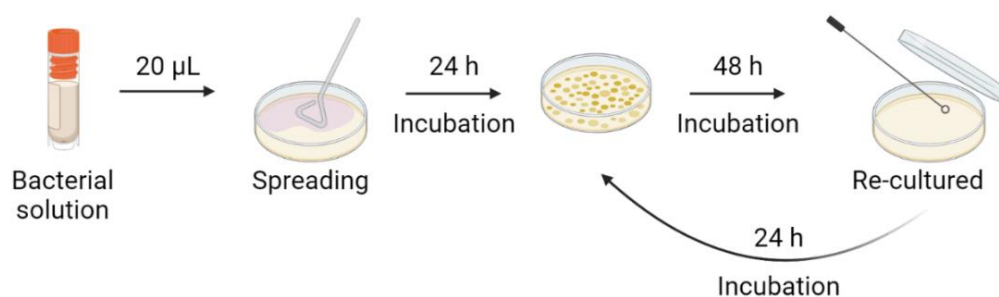


Figure 2.2: Representative schematic diagram to show the re-culture process.

2.4 Antimicrobial Activity Tests

Two bacterial colonies were taken and placed in 1 mL of solution in a vial: *E. coli* and *S. aureus* in LB media and *E. faecalis* in BHI media. The vials were placed inside the incubator at 37 °C for 15 h in stirring condition at 150 rpm. After this, re-culture is performed by placing 100 µL of the original bacterial solution in new mediq. After 4 h, the bacteria can be used, as they will have reached their exponential growth phase.

The bacterial concentration was obtained using the McFarland 0.5 Barium Sulphate Standard kit (Liofilmchem S.r.l., Italy). Following this we have an optical density (OD) of 0.5 corresponds to 1.5×10^8 CFU/mL. For the antimicrobial tests conducted a concentration of 10^5 CFU/ml was used and it was obtained by diluting the stock with 1:10 human pooled serum (CELLect, USA). Once the bacterial solution of 10^5 CFU/mL was prepared, 0.5 mL of this was added to each well containing a Ti-PDA-LL37.

Each well is then exposed to NIR light for 1.5 min, followed by 1 min of absence of light and then repeated the exposure for a total of 5 times. The laser used for this aim was NIR laser of 808 nm with a power density of 2 W/cm^2 (Roithner Laser Technik).

Afterwards, the 24-well plate is placed in incubator at 37°C, in stirring condition at 150 rpm for 15 h. After this period, the solutions contained in each well are diluted 100 times and plated on LB agar or BHI agar plates. Finally, after 24 h in an incubator at 37 °C, the colonies present in the plates are counted.

Furthermore, the minimum inhibitory concentration (MIC) was also determined using the microplate reader at 600 nm combined with plating and colony counting. The two methods were used together as the absorbance measurement alone would not have distinguished the bactericidal effect from the bacteriostatic one. Therefore, by also using the plating, the antimicrobial effect of the coating is verified.

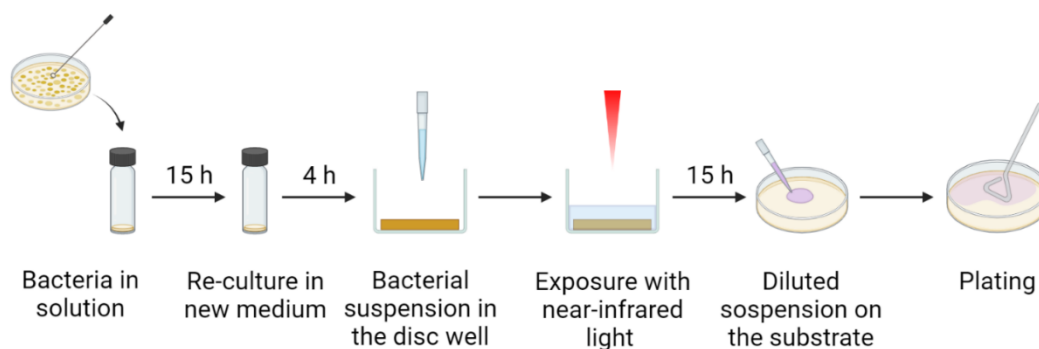


Figure 2.3: Representative schematic diagram to show the antimicrobial test.

2.5 Biofilm Tests

The bacteria used for this type of test are *S. aureus* and *E. faecalis*.

The preparation of the bacteria in solution is the same as in the antimicrobial activity tests. In the biofilm tests after 4 h from re-culture and after using the McFarland 0.5 Barium Sulphate Standard kit, the original solution is diluted with a solution made up of BHI medium and 2% glucose up to 10^6 CFU/mL. 0.5 mL of the bacterial solution was added in Ti-PDA-LL discs in 24-well plate, then it is exposed to NIR light similar to condition done for antimicrobial test. The plate is placed under static conditions in an incubator at 37 °C for 24 h.

After 24 h in the incubator, proceed with crystal violet staining to quantify the biofilm present on the surface of the disc. The solution present in each well is gently removed and rinsed with Milli-Q water. Wait for 1 h keeping the plate without lid in the incubator to allow drying. Then 0.5 mL of 0.2% crystal violet solution is placed in each well and waited for 10 min. After having gently removed the crystal violet, rinse with Milli-Q water. Put 0.5 mL of ethanol and acetone solution (80:20) and wait 10 min.

Finally, for biofilm quantification, 200 μ L from each well are placed in a transparent 96-well plate and the absorbance is measured at 590 nm using the spectrophotometer-microplate reader.

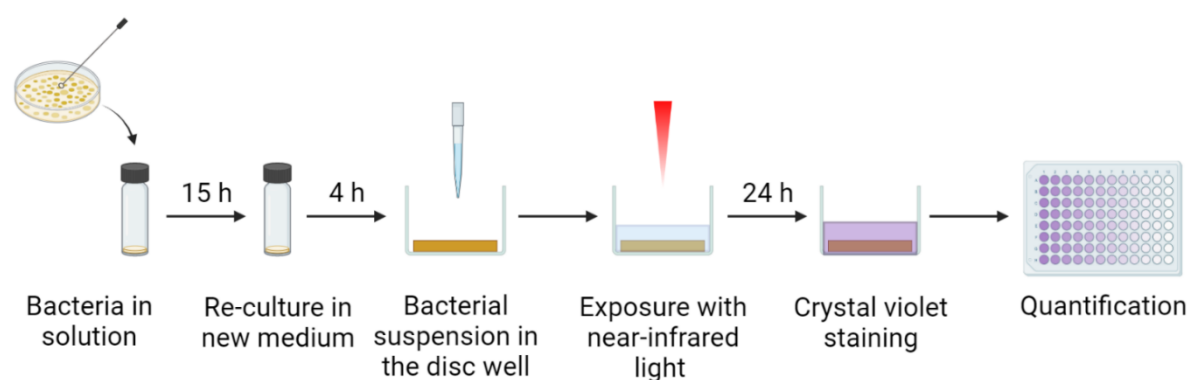


Figure 2.4: Representative schematic diagram to show the antibiofilm test.

2.7 Attenuated Total Reflectance – Fourier Transformed Infra-Red spectroscopy

The presence of the PDA coating was confirmed by the Attenuated total reflectance – Fourier transformed infra-red (ATR - FTIR) spectroscopy analysis. Analysis was performed using IRAffinity-1S (Shimadzu) equipped with a diamond crystal ATR accessory (QATR10).

2.8 Contact Angle

The samples used for the contact angle studies were analyzed immediately after opening and measurements were made at room temperature. An OCA 15 plus video-based optical contact angle measuring device equipped with an electronic syringe unit (Dataphysics Instruments GmbH, Germany) was used to perform the wettability studies. DDWs were used. Static contact angles were measured at room temperature by the sessile drop method, on 4 ml droplets for water deposited on the surface. At least 3 drops were used for each type of sample.

The contact angles were calculated by the SCA20 software (Dataphysics, version 2.0), adapting the fall profiles to the Young-Laplace equation.

2.9 Quartz Crystal Microbalance with Dissipation monitoring

The quartz crystal microbalance with dissipation (QCM-D) analysis was used to further characterize the coating in its various steps. The Q-Sense instrument (Biolin Scientific) was used together with the related Q-Sense Explorer System (QE 401 Electronics Unit, QCP 101 Chamber Platform). The sensor used is the Q-Sensor QSX 301 Gold. The temperature used to perform the entire acquisition is 25 °C.

2.10 X-Ray Photoelectron Spectroscopy

To evaluate the chemical composition of the obtained surface, X-Ray Photoelectron Spectroscopy (XPS) analysis (Scienta ESCA 200) was performed on Ti, PDA coated Ti, PDA-linker coated Ti and LL37-linker-PDA coated Ti surfaces.

2.11 Statistical Analysis

All tests were repeated at least three times to ensure the repeatability of the results.

All results are reported as average \pm SEM. All data were analyzed with GraphPad software (GraphPad 9, La Jolla, USA). Tukey's multiple comparisons one-way ANOVA test was used with the following specifications: **** P < 0.0001, *** P < 0.001, ** P < 0.01, * P < 0.05 and ns \geq 0.5.

Chapter 3

Results and discussion

3.1 Polydopamine coating and characterization

Different concentrations of dopamine were used to do coating on Ti discs in order to find the best condition providing the uniform PDA coating. It is found that 260 mM dopamine concentration was optimum to do uniform and thicker coatings on Ti discs as observed in UV-vis spectra (Figure 3.1A and 3.1B).

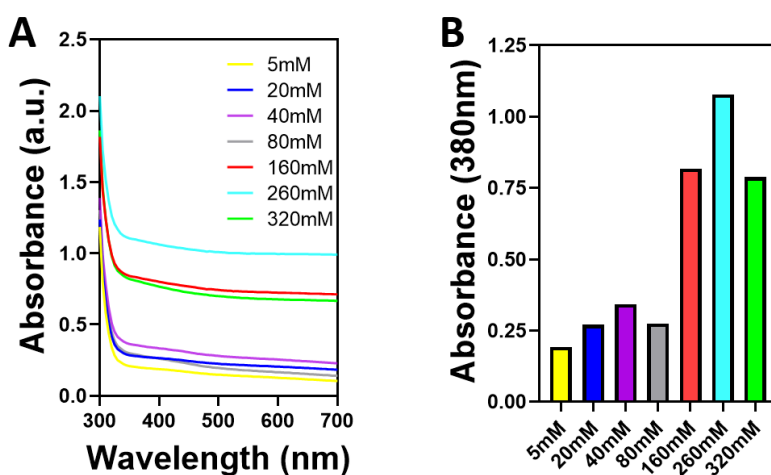


Figure 3.1: (A) UV-vis spectra of PDA coated Ti discs (B) Absorbance at 380 nm of different concentrations of PDA coated Ti discs.

After selecting the best concentration of dopamine, a faster coating method is tried to obtain the uniform coating in a shorter time, passing from 15 h to 1 h. Clear differences between the two methods can be seen in Figure 3.2A, 3.2B and 3.2C. In addition to the aspect, the absorbance of Ti-PDA obtained with the different methods was also measured (Figure 3.2D).

Although the coating was observed using ultrafast method, the thickness of PDA layer on Ti discs was not sufficient and uniform. We could also observe the Ti surface (Figure 3.2B).

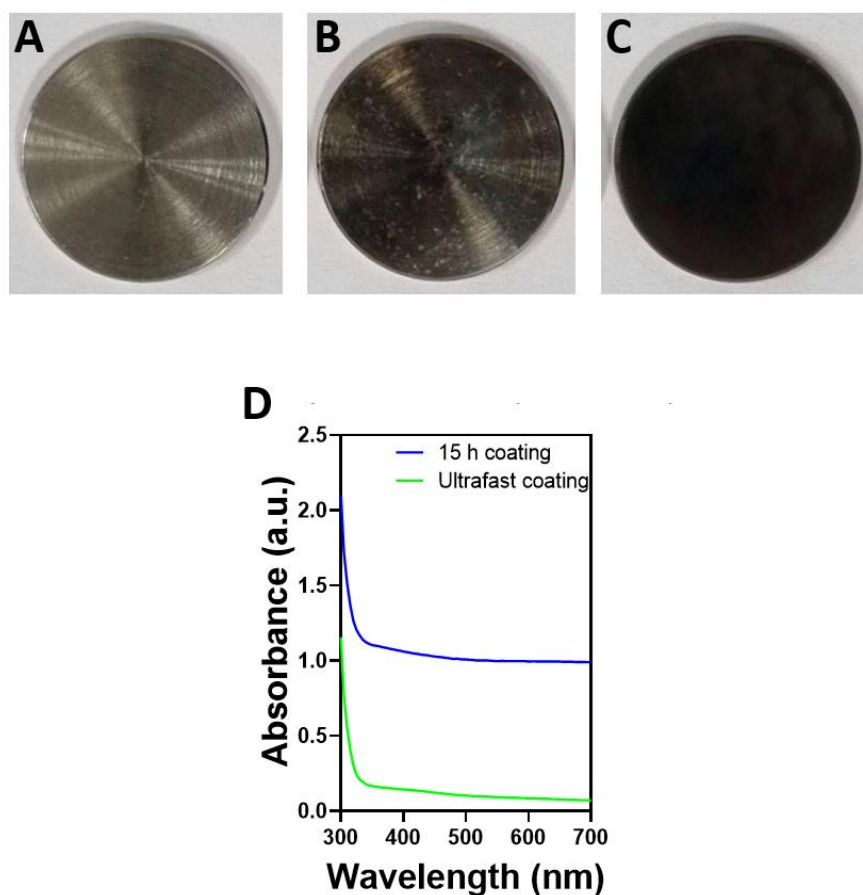


Figure 3.2: Comparison between PDA coating methods. (A) Ti disc. (B) Ti disc coated with ultrafast method. (C) Ti disc coated with 15 h method. (D) Absorbance at different wavelengths.

The presence of the PDA coating was confirmed by ATR - FTIR spectroscopic analysis (Figure 3.3A). The presence of the CH group is confirmed by the peak at 1280 cm^{-1} and that of the NH group by the following peak at 1500 cm^{-1} . It is also possible to see the peak corresponding to the OH group at 3100 cm^{-1} .

The stability of the PDA coating in solution was also evaluated. The Ti-PDA disc was placed in 1 mL of Milli-Q water for 48 h. Figure 3.1.3B shows the absorbance of Milli-Q water before and after 48 h together with the absorbance of the starting coating. There is no leaching of PDA from the surfaces after 48 h of incubation in water, indicating that PDA coating is stable (Figure 3.3B).

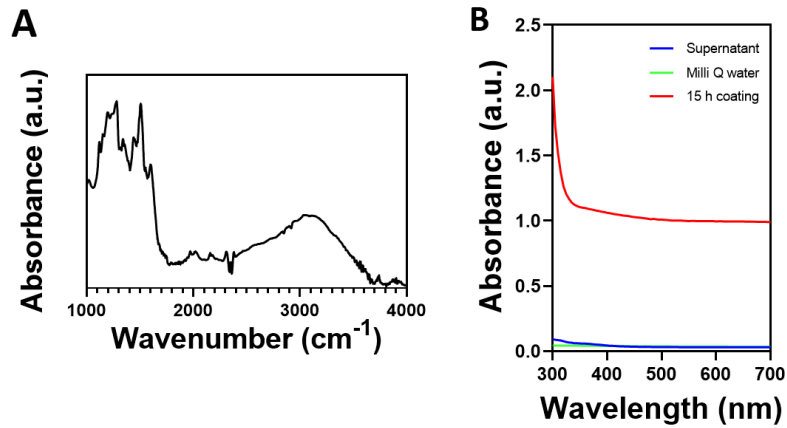


Figure 3.3: Presence and stability of the PDA coating. (A) ATR – FTIR spectrum of Ti-PDA disc. (B) Stability of the PDA coating in solution.

The surface wettability behavior was characterized by measuring the contact angle (Figure 3.4). The Ti-PDA surface is extremely hydrophilic with a contact angle around 5°. Then we proceeded by measuring the contact angle of the Ti-PDA-LL37 surface. The angle measured on the final surface is about 30°, indicating the conjugation of LL37 peptide on the surface of PDA-Ti.

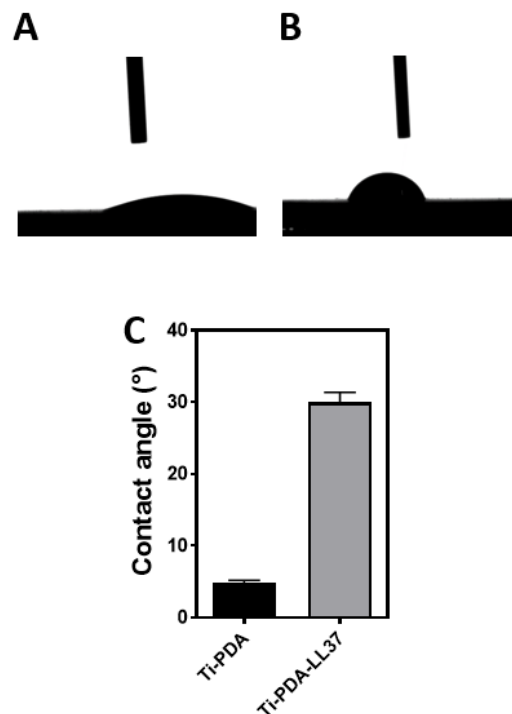


Figure 3.4: Contact angle. A) Image of the water drop on the Ti-PDA surface. B) Image of the water drop on the Ti-PDA-LL37 surface. C) Quantification of the contact angle of Ti-PDA and Ti-PDA-LL37.

Furthermore, the amount of conjugated peptide on the surface was calculated using the Lambert-Beer law and $35 \pm 3 \mu\text{g}/\text{cm}^2$ was obtained.

The QCM-D analysis was finally performed to further characterize the various coating steps. In Figure 3.5 it is possible to identify 3 steps in the trend of the frequency variation and dissipation variation curves. The first was due to the deposition of PDA on the surface for 15 hours (A-B). We note a variation of the frequency combined with a not too evident dissipation, this suggests that the deposited material is not very soft but rather rigid. The second step is due to the deposition of the NH_2 -PEG-MAL linker for 1.5 hours (B-C). A frequency variation suggests an increase in mass and there is also an increase in the dissipation variation, therefore a softer material than PDA is bonded. Finally, LL37 is bound to the surface causing the last trend of the curves (C-D). The peptide binding to the surface will lead to a further increase in mass as can be seen from the frequency variation but also to an increase in the dissipation variation caused by its softer nature.

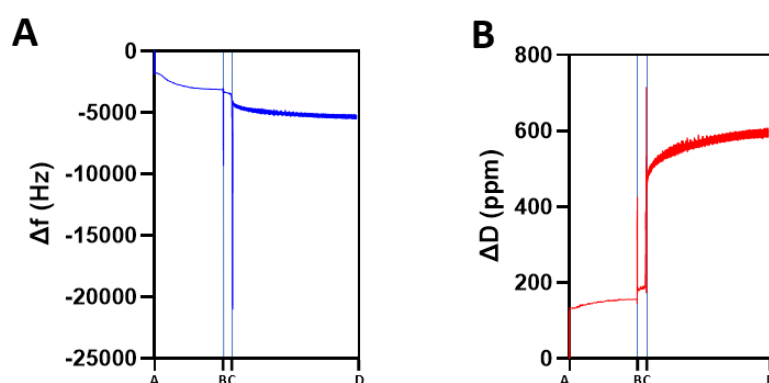
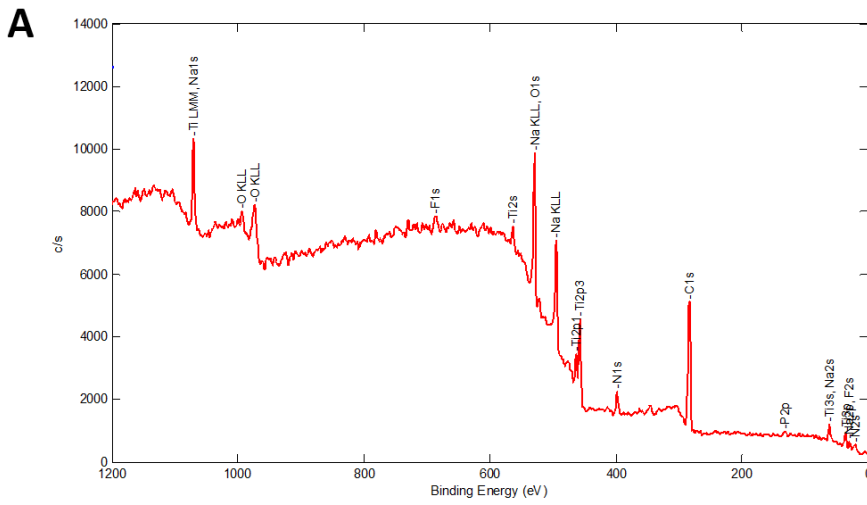
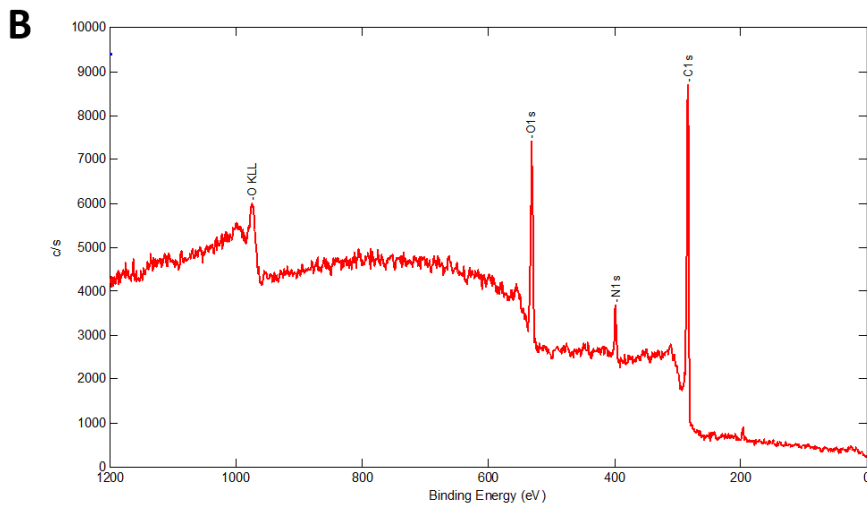


Figure 3.5: QCM-D monitoring performed on Ti-PDA-LL37 surfaces. A) Frequency variation curve. B) Dissipation variation curve.

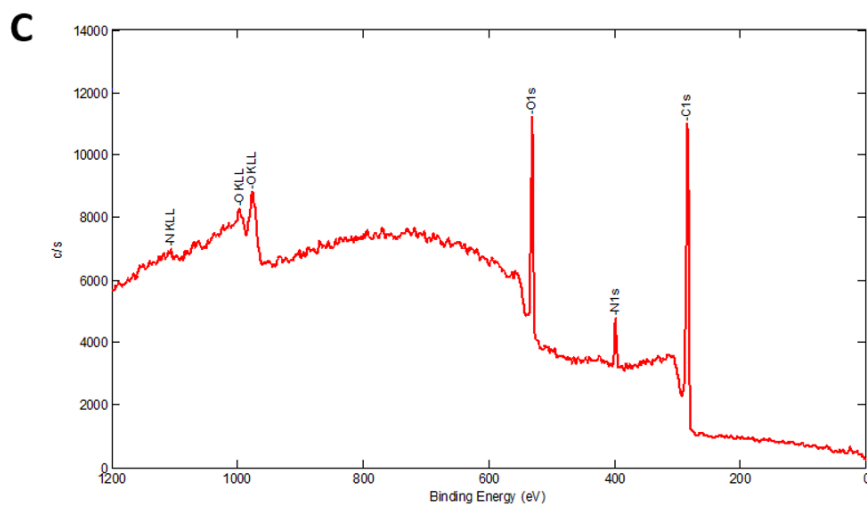
From the XPS analysis of the Ti disc after cleaning with NaOH it can be seen that there are peaks for Ti but also C, O and Na (Figure 3.6A). Analyzing the Ti-PDA surface, characteristic peaks of polyDOPA are noted, more precisely C, O and N with an increase in the C peak compared to the Ti disc alone (Figure 3.6B). As far as the Ti-PDA surface functionalized with linker is concerned, the same peaks of the Ti-PDA are recognized (Figure 3.6C). Finally, the Ti-PDA-LL37 surface shows in addition to the C, O and N peaks also P, Na and S (Figure 3.6D).



Surface elemental compositions (%)	
C 1s	50,3
O 1s	24,4
Na 1s	9,1
N 1s	6,0
Ti 2p	5,1
F 1s	3,7
P 2p	1,4



Surface elemental compositions (%)	
C 1s	73,2
O 1s	20,1
N 1s	6,7



Surface elemental compositions (%)	
C 1s	72,0
O 1s	21,5
N 1s	6,5

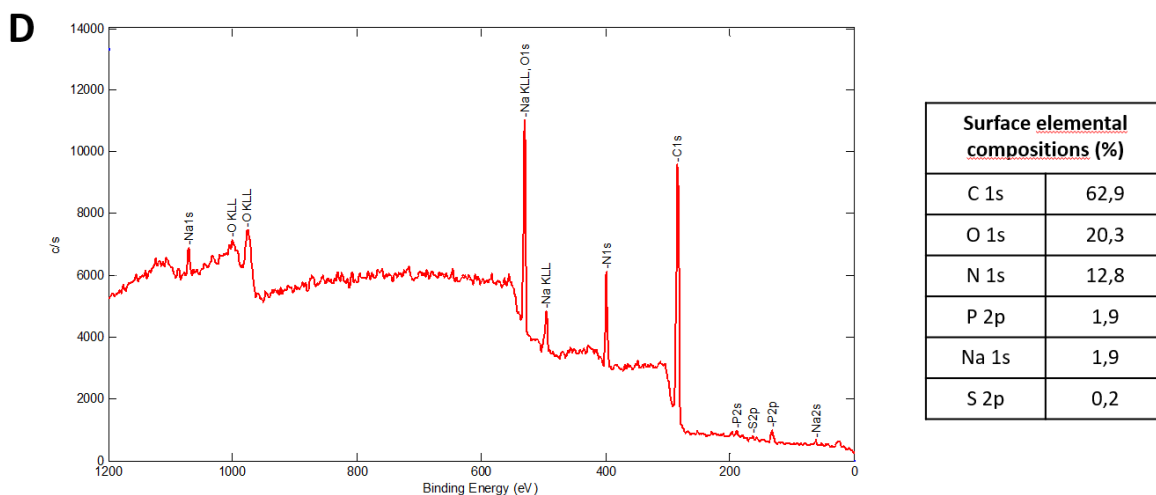


Figure 3.6: XPS analysis. A) Ti disc after cleaning. B) Ti-PDA surface. C) Ti-PDA-linker surface. D) Ti-PDA-LL37 surface.

3.2 NIR laser measurements

To optimize the laser power density, NIR laser was exposed to Ti-PDA discs at different powers such as 0.5, 1, 1.5 and 2 W/cm². The Ti-PDA disc was exposed to the laser for 5 min and then waited until the temperature returned to the starting temperature. The measured temperature is that of the solution where the disc was immersed and was measured every 30 s (Figure 3.7A). It is found that show coating (15h) of PDA on Ti discs produce high temperature rise than the ultrafast coated Ti-PDA discs (Figure 3.7B).

The temperature increases during 1.5 min exposures for 5 cycles and the 1 min break were also measured. Again, the temperature was measured on the surface of the Ti-PDA disc in solution every 30 s (Figure 3.7C). It is found that the temperature increased during the exposure and decreased once the laser was switched off (Figure 3.7C).

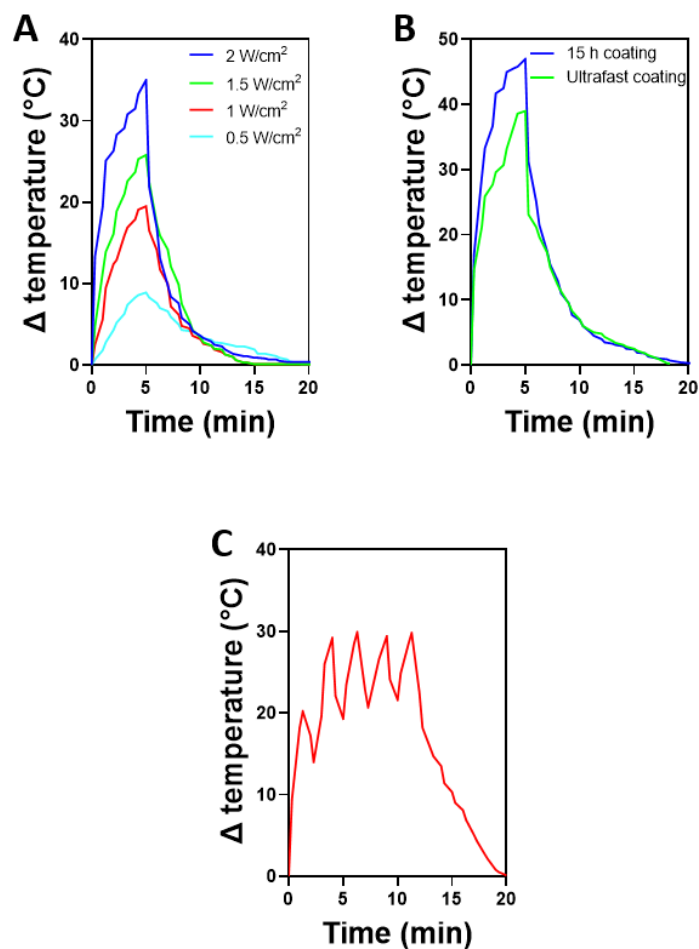


Figure 3.7: Evaluation of photothermal property of Ti-PDA discs. (A) Estimation of temperature increase after exposure of different laser power densities. (B) Comparison between 15 h coating and ultrafast coating. (C) The cycle of laser switch-on and switch off to evaluate the temperature.

3.4 Antimicrobial Activity Tests

3.4.1 Determination of the MIC of LL37

The MIC for LL37 free peptide was determined by testing five different concentrations of the peptide: 4, 6, 8, 10 and 12 $\mu\text{g}/\text{mL}$ against *E. coli*. Similarly, the MIC of LL37 peptide against *S. aureus* was determined using different concentration of LL37 such as 4, 6, 8, 12 and 20 $\mu\text{g}/\text{mL}$. These concentrations were evaluated against 10^5 CFU/mL of both bacteria.

It can be observed that the increasing concentration of LL37 peptides retarded the growth of *E. coli*, and 12 $\mu\text{g}/\text{mL}$ of LL37 peptide completely killed the bacteria (Figure 3.8A). In the graph relating to the plating method (Figure 3.8B) it is again noted that no growth of bacteria is seen when 12 $\mu\text{g}/\text{mL}$ of LL37 peptides is exposed to bacteria.

On the other hand, it can be seen that 12 and 20 $\mu\text{g}/\text{mL}$ seem to be effective to prevent the growth of *S. aureus* (Figure 3.8C). If the graph relating to the plating method (Figure 3.8D) is also taken into consideration, however, it can be noted that no growth is recorded only in the case of 20 $\mu\text{g}/\text{mL}$.

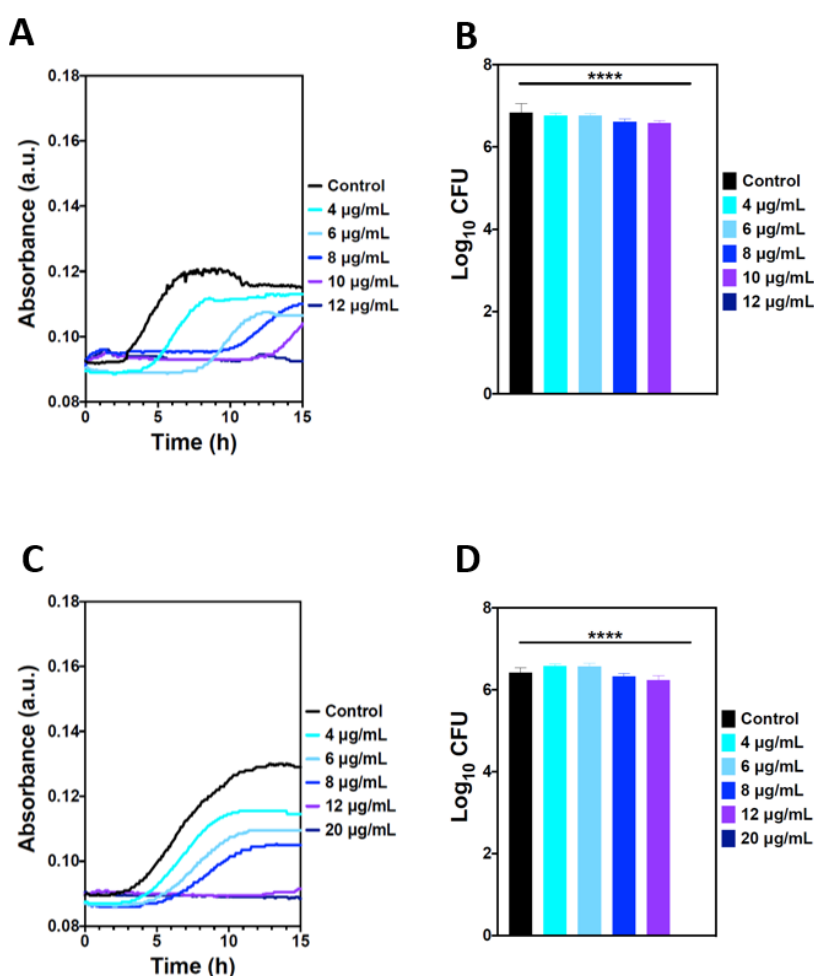


Figure 3.8: Determination of the MIC of LL37. (A) Different growth kinetics of *E. coli* under LL37 concentrations. (B) Antimicrobial activity of different concentrations of LL37 recorded with the plating method against *E. coli*. (C) Different growth kinetics of *S. aureus* under LL37 concentrations. (D) Antimicrobial activity of different concentrations of LL37 recorded with the plating method against *S. aureus*.

3.4.2 Antimicrobial effect

In general, Figure 3.8 shows the coatings containing CuCl_2 are more effective as antimicrobial effect. We noted that the survival of *E. coli* in the presence of Cu ions only in the case of PDA coating only without the exposure of the laser. On the other hand, without the use of Cu ions, there is almost no survival of *E. coli* only in the case of Ti-PDA-LL37 with the use of laser (Figure 3.9B).

As with *S. aureus*, when there is Cu ions in the coating, the same pattern is seen as with *E. coli* (Figure 3.9C). On the other hand, in the case of Cu ions-free coating, survival is seen only in the case of PDA and LL peptides again without laser exposure (Figure 3.9D).

In the case of *E. faecalis* the results obtained are different from the two previous cases. In the presence of Cu ions, there is no survival in the case of PDA and PDA coated with LL37 peptides with the laser exposure. When Cu ions are not used, survival is not only achieved in the case of PDA coating combined with the laser exposure. This result suggests that the antimicrobial peptide is not effective in these conditions even when combined with the laser exposure.

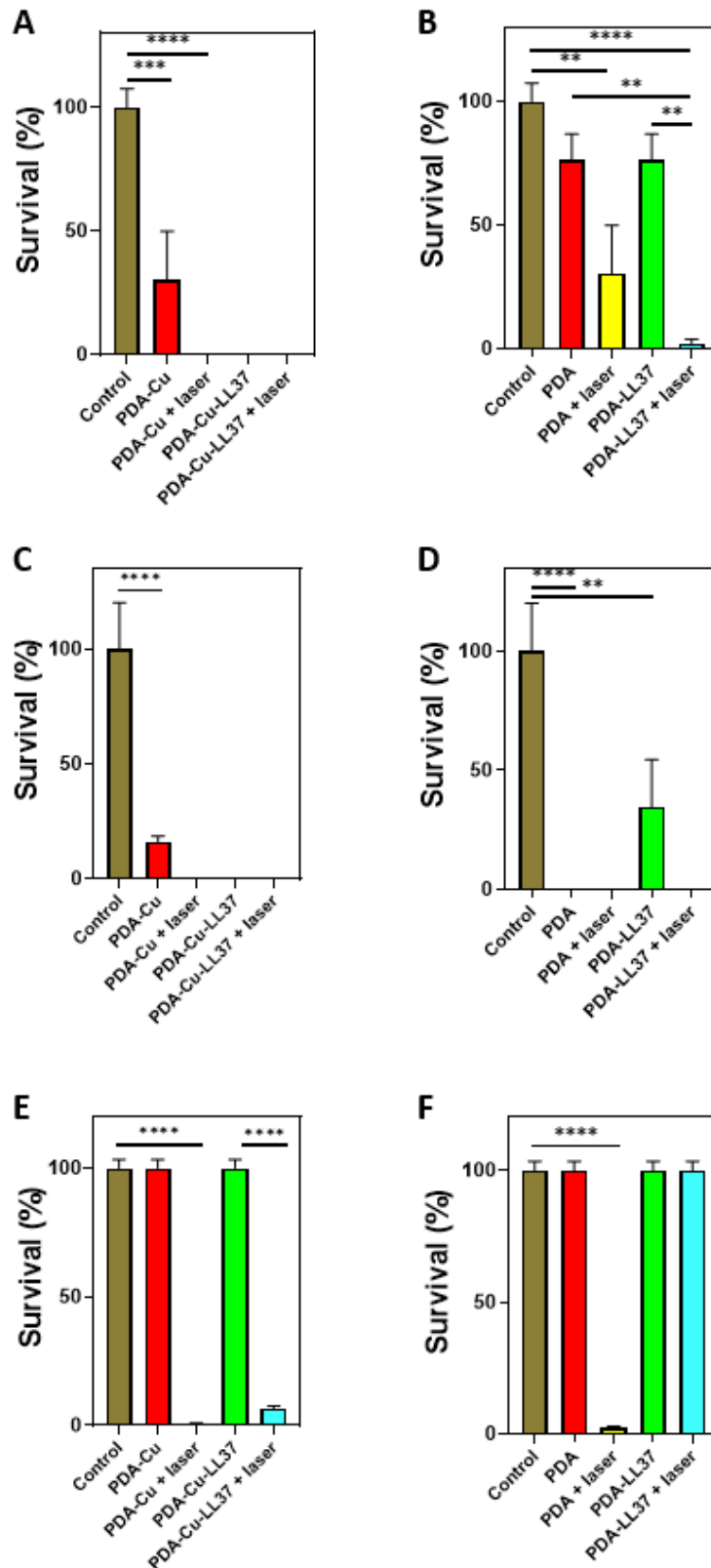


Figure 3.9: Results of antimicrobial tests. (A) *E. coli* survival rate in presence of CuCl_2 as the first step of the coating. (B) *E. coli* survival rate without the use of CuCl_2 . (C) *S. aureus* survival rate in presence of CuCl_2 as the first step of the coating. (D) *S. aureus* survival rate without the use of CuCl_2 . (E) *E. faecalis* survival rate in presence of CuCl_2 as the first step of the coating. (F) *E. faecalis* survival rate without the use of CuCl_2 .

3.5 Biofilm Tests

For the antibiofilm activity, Cu ions-free PDA coatings were used against *S. aureus* and *E. faecalis*.

Good antibiofilm activities were achieved with both *S. aureus* (Figure 3.10A) and *E. faecalis* (Figure 3.10B) using Ti-PDA-LL37 discs with laser exposure. However, antibiofilm properties were also observed for other conditions where laser was not exposed. It is possible to visually notice the effect of the coating with respect to untreated discs in Figure 11. The violet color is clearly present on the entire surface of the untreated discs, instead on the Ti-PDA-LL37 discs both in the case of *S. aureus* and in the case of *E. faecalis* the purplish color is not observed.

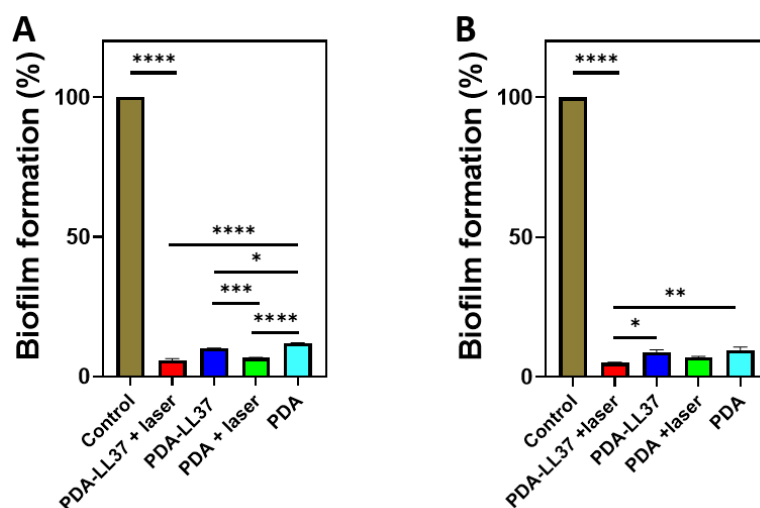


Figure 3.10: Results of biofilm tests. (A) Percentage of *S. aureus* biofilm formed under different conditions. (B) Percentage of *E. faecalis* biofilm formed under different conditions.

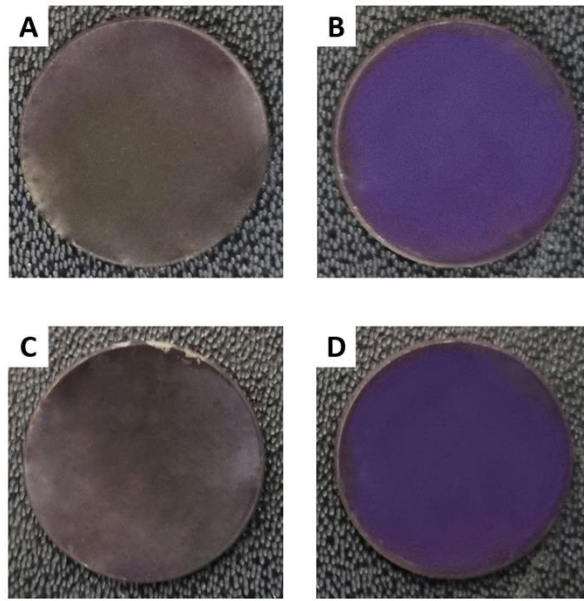


Figure 3.11: Discs after crystal violet staining. A) Ti-PDA-LL37 after biofilm test with *S. aureus*. B) Untreated Ti disc after biofilm test with *S. aureus*. C) Ti-PDA-LL37 after biofilm test with *E. faecalis*. D) Untreated Ti disc after biofilm test with *E. faecalis*.

Chapter 4

Conclusions and Outlook

A multifunctional coating on titanium surface was developed by combining the photothermal property of PDA upon NIR laser and the antimicrobial property of LL37 peptides. The optimum condition was developed to do uniform coating of PDA on titanium surface. 260 mM dopamine and 15 h of incubation is required to produce PDA coated Ti surfaces. PDA coated Ti surfaces were further conjugated with LL37 peptides using amine-PEG-maleimide linker. Maleimide group of linker reacts with thiol group of LL37 peptide through maleimide-thiol reaction.

The Ti-PDA-LL37 surface have potent antimicrobial activity against Gram-positive and Gram-negative bacteria in all tested conditions. More precisely, a high antibacterial activity was recorded against *E. Coli* and *S. aureus* in planktonic form with the use of NIR laser. on the other hand, against *E. faecalis*, the good antimicrobial results were obtained only in the presence of Cu ions coated PDA discs with the aid of NIR light. This aspect is interesting and in the future it would be important to evaluate the effect of this coatings on cytotoxicity

As for the biofilm tests, Ti-PDA-LL37 without Cu ions in the coating recorded very low values of adhesion and biofilm formation. This result is important because if the developed coating does not favor adhesion by the bacteria, they will not be able to put the implant at risk by causing an infection in the site.

Given and confirmed the antimicrobial efficacy, the subsequent verification of biocompatibility and therapeutic efficacy is necessary in vitro and in vivo models. The properties of LL37 peptides such as osteogenesis and wound healing could prove extremely useful in the case of a dental implant for antibiotic-free healing and without the development of infections.

The coating developed in this project could be used as a novel and valid strategy in the dental field to combat and prevent the development of peri-implantitis with possible beneficial effects on the tissues surrounding the implant.

Bibliography

- [1] W. Zhang and P. C. Yelick, "Tooth Repair and Regeneration: Potential of Dental Stem Cells," *Trends in Molecular Medicine*, vol. 27, no. 5, pp. 501–511, 2021, doi: 10.1016/j.molmed.2021.02.005.
- [2] <https://www.nidcr.nih.gov/research/data-statistics/tooth-loss/adults>.
- [3] M. Doria and R. Buzzetti, "Osservazioni sulle Linee Guida Nazionali per la promozione della salute orale e la prevenzione delle patologie orali in età evolutiva," *Medico e Bambino*, vol. 29, no. 3, pp. 161–164, 2010.
- [4] <https://www.treccani.it/enciclopedia/parodonto/>.
- [5] <https://newsinhealth.nih.gov/2019/05/mouth-microbes>.
- [6] <https://www.treccani.it/enciclopedia/tartaro-dentario/>.
- [7] D. Clark and L. Levin, "In the dental implant era, why do we still bother saving teeth?," *Dental Traumatology*, vol. 35, no. 6, pp. 368–375, 2019, doi: 10.1111/edt.12492.
- [8] <https://biorender.com/>.
- [9] B. Guillaume, "Les implants dentaires : revue," *Morphologie*, vol. 100, no. 331, pp. 189–198, 2016, doi: 10.1016/j.morpho.2016.02.002.
- [10] V. Babuska, O. Moztarzadeh, T. Kubikova, A. Moztarzadeh, D. Hrusak, and Z. Tonar, "Evaluating the osseointegration of nanostructured titanium implants in animal models: Current experimental methods and perspectives (Review)," *Biointerphases*, vol. 11, no. 3, p. 030801, 2016, doi: 10.1116/1.4958793.
- [11] K. U. Dmd, "Effects of Chemical and Prophylactic Agents Used in Dentistry on Titanium Implant Surfaces," 2013.
- [12] K. Liaw, R. H. Delfini, and J. J. Abrahams, "Dental Implant Complications," *Seminars in Ultrasound, CT and MRI*, vol. 36, no. 5, pp. 427–433, 2015, doi: 10.1053/j.sult.2015.09.007.
- [13] O. Camps-Font, P. Martín-Fatás, A. Clé-Ovejero, R. Figueiredo, C. Gay-Escoda, and E. Valmaseda-Castellón, "Postoperative infections after dental implant placement: Variables

- associated with increased risk of failure," *Journal of Periodontology*, vol. 89, no. 10, pp. 1165–1173, 2018, doi: 10.1002/JPER.18-0024.
- [14] F. Schwarz, J. Derks, A. Monje, and H. L. Wang, "Peri-implantitis," *Journal of periodontology*, vol. 89, no. September 2017, pp. S267–S290, 2018, doi: 10.1002/JPER.16-0350.
- [15] A. Monje, R. Pons, A. Rocuzzo, G. E. Salvi, and J. Nart, "Reconstructive therapy for the management of peri-implantitis via submerged guided bone regeneration: A prospective case series," *Clinical Implant Dentistry and Related Research*, vol. 22, no. 3, pp. 342–350, 2020, doi: 10.1111/cid.12913.
- [16] L. J. A. Heitz-Mayfield and G. E. Salvi, "Peri-implant mucositis," *Journal of Clinical Periodontology*, vol. 45, no. July 2016, pp. S237–S245, 2018, doi: 10.1111/jcpe.12953.
- [17] "imm periimpl." <https://360imaging.com/peri-implantitis-what-causes-implant-failure/>.
- [18] Z. Liu, X. Liu, and S. Ramakrishna, "Surface engineering of biomaterials in orthopedic and dental implants: Strategies to improve osteointegration, bacteriostatic and bactericidal activities," *Biotechnology Journal*, vol. 16, no. 7, pp. 1–23, 2021, doi: 10.1002/biot.202000116.
- [19] Z. Xu *et al.*, "Application of totarol as natural antibacterial coating on dental implants for prevention of peri-implantitis," *Materials Science and Engineering C*, vol. 110, no. January, p. 110701, 2020, doi: 10.1016/j.msec.2020.110701.
- [20] E. Tambone *et al.*, "Rhamnolipid coating reduces microbial biofilm formation on titanium implants: an in vitro study," *BMC Oral Health*, vol. 21, no. 1, pp. 1–13, 2021, doi: 10.1186/s12903-021-01412-7.
- [21] H. Geng *et al.*, "Engineered chimeric peptides with antimicrobial and titanium-binding functions to inhibit biofilm formation on Ti implants," *Materials Science and Engineering C*, vol. 82, no. August 2017, pp. 141–154, 2018, doi: 10.1016/j.msec.2017.08.062.
- [22] C. Mas-Moruno, B. Su, and M. J. Dalby, "Multifunctional Coatings and Nanotopographies: Toward Cell Instructive and Antibacterial Implants," *Advanced Healthcare Materials*, vol. 8, no. 1, 2019, doi: 10.1002/adhm.201801103.
- [23] G. M. Esteves, J. Esteves, M. Resende, L. Mendes, and A. S. Azevedo, "Antimicrobial and Antibiofilm Coating of Dental Implants—Past and New Perspectives," *Antibiotics*, vol. 11, no. 2, pp. 1–15, 2022, doi: 10.3390/antibiotics11020235.
- [24] F. Chen, C. Liu, and Y. Mao, "Bismuth-doped injectable calcium phosphate cement with

- improved radiopacity and potent antimicrobial activity for root canal filling,” *Acta Biomaterialia*, vol. 6, no. 8, pp. 3199–3207, 2010, doi: 10.1016/j.actbio.2010.02.049.
- [25] H. Chouirfa, H. Bouloussa, V. Migonney, and C. Falentin-Daudré, “Review of titanium surface modification techniques and coatings for antibacterial applications,” *Acta Biomaterialia*, vol. 83, pp. 37–54, 2019, doi: 10.1016/j.actbio.2018.10.036.
- [26] A. S. K. Kiran, T. S. S. Kumar, R. Sanghavi, M. Doble, and S. Ramakrishna, “Antibacterial and bioactive surface modifications of titanium implants by PCL/TiO₂ nanocomposite coatings,” *Nanomaterials*, vol. 8, no. 10, 2018, doi: 10.3390/nano8100860.
- [27] P. Liu, Y. Hao, Y. Zhao, Z. Yuan, Y. Ding, and K. Cai, “Surface modification of titanium substrates for enhanced osteogenetic and antibacterial properties,” *Colloids and Surfaces B: Biointerfaces*, vol. 160, pp. 110–116, 2017, doi: 10.1016/j.colsurfb.2017.08.044.
- [28] T. Nichol *et al.*, “The antimicrobial activity and biocompatibility of a controlled gentamicin-releasing single-layer sol-gel coating on hydroxyapatite-coated titanium,” *Bone and Joint Journal*, vol. 103 B, no. 3, pp. 522–529, 2021, doi: 10.1302/0301-620X.103B3.BJJ-2020-0347.R1.
- [29] K. Bazaka, M. V. Jacob, W. Chrzanowski, and K. Ostrikov, “Anti-bacterial surfaces: Natural agents, mechanisms of action, and plasma surface modification,” *RSC Advances*, vol. 5, no. 60, pp. 48739–48759, 2015, doi: 10.1039/c4ra17244b.
- [30] J. G. S. Souza, M. M. Bertolini, R. C. Costa, B. E. Nagay, A. Dongari-Bagtzoglou, and V. A. R. Barão, “Targeting implant-associated infections: titanium surface loaded with antimicrobial,” *iScience*, vol. 24, no. 1, 2021, doi: 10.1016/j.isci.2020.102008.
- [31] S. Anhydride, S. Tespsa, J. Buxadera-palomero, M. Godoy-gallardo, and M. Molmeneu, “TSP SILANE Antibacterial Properties of Triethoxysilylpropyl,” pp. 1–15.
- [32] M. K. Ji *et al.*, “Evaluation of antibacterial activity and osteoblast-like cell viability of TiN, ZrN and (Ti_{1-x}Zr_x)N coating on titanium,” *Journal of Advanced Prosthodontics*, vol. 7, no. 2, pp. 166–171, 2015, doi: 10.4047/jap.2015.7.2.166.
- [33] D. Lauritano, C. A. Bignozzi, D. Pazzi, F. Cura, and F. Carinci, “Efficacy of a new coating of implantabutment connections in reducing bacterial loading: An in vitro study,” *ORAL and Implantology*, vol. 10, no. 1, pp. 1–10, 2017, doi: 10.11138/orl/2017.10.1.001.
- [34] P. C. Zamecnik and M. L. Stephenson, “Inhibition of Rous sarcoma virus replication and cell transformation by a specific oligodeoxynucleotide,” *Proceedings of the National Academy of*

- Sciences of the United States of America*, vol. 75, no. 1, pp. 280–284, 1978, doi: 10.1073/pnas.75.1.280.
- [35] B. F. Baker and B. P. Monia, “Novel mechanisms for antisense-mediated regulation of gene expression,” *Biochimica et Biophysica Acta - Gene Structure and Expression*, vol. 1489, no. 1, pp. 3–18, 1999, doi: 10.1016/S0167-4781(99)00146-3.
- [36] J. König, K. Zarnack, N. M. Luscombe, and J. Ule, “and Perspectives,” vol. 13, no. February, pp. 77–83, 2012.
- [37] R. M. Dedrick *et al.*, “Engineered bacteriophages for treatment of a patient with a disseminated drug-resistant *Mycobacterium abscessus*,” *Nature Medicine*, vol. 25, no. 5, pp. 730–733, 2019, doi: 10.1038/s41591-019-0437-z.
- [38] K. Kingwell, “Bacteriophage therapies re-enter clinical trials,” *Nature Reviews Drug Discovery*, vol. 14, no. 8, pp. 515–516, 2015, doi: 10.1038/nrd4695.
- [39] S. Kaur, K. Harjai, and S. Chhibber, “Bacteriophage mediated killing of *Staphylococcus aureus* in vitro on orthopaedic K wires in presence of linezolid prevents implant colonization,” *PLoS ONE*, vol. 9, no. 3, pp. 1–10, 2014, doi: 10.1371/journal.pone.0090411.
- [40] P. Georgios E. Romanos DDS, PhD, Prof. Dr. med. dent, Fawad Javed BDS, PhD, Rafael Arcesio Delgado-Ruiz DDS, MSc, PhD, José Luis Calvo-Guirado DDS, MS, “Peri-implant Diseases: A Review of Treatment Interventions,” *Dental Clinics of North America*, vol. 59, no. 1, pp. 157–178, 2015, doi: 10.1016/j.cden.2014.08.002.
- [41] N. O. Fabio Camacho-Alonso, Jesús Salinas, Mariano Sánchez-Siles, Jesús Pato-Mourelo, Brian Davis Cotrina-Veizaga, “Synergistic antimicrobial effect of photodynamic therapy and chitosan on the titanium-adherent biofilms of *Staphylococcus aureus*, *Escherichia coli*, and *Pseudomonas aeruginosa*: An in vitro study,” *Journal of Periodontology*, vol. 93, no. 6, pp. e104–e115, 2021, doi: 10.1002/JPER.21-0306.
- [42] Z. Yuan *et al.*, “Biocompatible MoS₂/PDA-RGD coating on titanium implant with antibacterial property via intrinsic ROS-independent oxidative stress and NIR irradiation,” *Biomaterials*, vol. 217, no. March, 2019, doi: 10.1016/j.biomaterials.2019.119290.
- [43] F. Cieplik, “The dental plaque biofilm matrix,” vol. 86, no. 1, pp. 32–56, 2022, doi: 10.1111/prd.12361.The.
- [44] S. Manna, C. Ghanty, P. Baidara, T. K. R. Barik, and S. M. Mandal, “Electrochemical communication in biofilm of bacterial community,” *Journal of Basic Microbiology*, vol. 60, no.

- 10, pp. 819–827, 2020, doi: 10.1002/jobm.202000340.
- [45] C. Solano, M. Echeverz, and I. Lasa, “Biofilm dispersion and quorum sensing,” *Current Opinion in Microbiology*, vol. 18, no. 1, pp. 96–104, 2014, doi: 10.1016/j.mib.2014.02.008.
- [46] M. Comune *et al.*, “Antimicrobial peptide-gold nanoscale therapeutic formulation with high skin regenerative potential,” *Journal of Controlled Release*, vol. 262, no. July, pp. 58–71, 2017, doi: 10.1016/j.jconrel.2017.07.007.
- [47] M. Mahlapuu, C. Björn, and J. Ekblom, “Antimicrobial peptides as therapeutic agents: opportunities and challenges,” *Critical Reviews in Biotechnology*, vol. 40, no. 7, pp. 978–992, 2020, doi: 10.1080/07388551.2020.1796576.
- [48] S. T. Henriques *et al.*, “Redesigned Spider Peptide with Improved Antimicrobial and Anticancer Properties,” *ACS Chemical Biology*, vol. 12, no. 9, pp. 2324–2334, 2017, doi: 10.1021/acscchembio.7b00459.
- [49] C. K. Wang and D. J. Craik, “Designing macrocyclic disulfide-rich peptides for biotechnological applications perspective,” *Nature Chemical Biology*, vol. 14, no. 5, pp. 417–427, 2018, doi: 10.1038/s41589-018-0039-y.
- [50] M. Pushpanathan, P. Gunasekaran, and J. Rajendhran, “Antimicrobial peptides: Versatile biological properties,” *International Journal of Peptides*, vol. 2013, no. Table 1, 2013, doi: 10.1155/2013/675391.
- [51] A. Bin Hafeez, X. Jiang, P. J. Bergen, and Y. Zhu, “Antimicrobial peptides: An update on classifications and databases,” *International Journal of Molecular Sciences*, vol. 22, no. 21, 2021, doi: 10.3390/ijms222111691.
- [52] R. Geitani, C. A. Moubareck, Z. Xu, D. Karam Sarkis, and L. Touqui, “Expression and Roles of Antimicrobial Peptides in Innate Defense of Airway Mucosa: Potential Implication in Cystic Fibrosis,” *Frontiers in Immunology*, vol. 11, no. June, pp. 1–11, 2020, doi: 10.3389/fimmu.2020.01198.
- [53] J. P. Tam, S. Wang, K. H. Wong, and W. L. Tan, “Antimicrobial peptides from plants,” *Pharmaceuticals*, vol. 8, no. 4, pp. 711–757, 2015, doi: 10.3390/ph8040711.
- [54] J. A. Masso-Silva and G. Diamond, “Antimicrobial peptides from fish,” *Pharmaceuticals*, vol. 7, no. 3, pp. 265–310, 2014, doi: 10.3390/ph7030265.
- [55] E. Cascales *et al.*, “Colicin Biology,” *Microbiology and Molecular Biology Reviews*, vol. 71, no. 1, pp. 158–229, 2007, doi: 10.1128/mmbr.00036-06.

- [56] E. M. Kościuczuk *et al.*, "Cathelicidins: family of antimicrobial peptides. A review.," *Molecular biology reports*, vol. 39, no. 12, pp. 10957–10970, 2012, doi: 10.1007/s11033-012-1997-x.
- [57] H. Y. Yi, M. Chowdhury, Y. D. Huang, and X. Q. Yu, "Insect antimicrobial peptides and their applications," *Applied Microbiology and Biotechnology*, vol. 98, no. 13, pp. 5807–5822, 2014, doi: 10.1007/s00253-014-5792-6.
- [58] S. Ramazi, N. Mohammadi, A. Allahverdi, E. Khalili, and P. Abdolmaleki, "A review on antimicrobial peptides databases and the computational tools," *Database*, vol. 2022, no. October 2021, pp. 1–17, 2022, doi: 10.1093/database/baac011.
- [59] M. Mahlapuu, J. Håkansson, L. Ringstad, and C. Björn, "Antimicrobial peptides: An emerging category of therapeutic agents," *Frontiers in Cellular and Infection Microbiology*, vol. 6, no. DEC, pp. 1–12, 2016, doi: 10.3389/fcimb.2016.00194.
- [60] H. Fedders, R. Podschun, and M. Leippe, "The antimicrobial peptide Ci-MAM-A24 is highly active against multidrug-resistant and anaerobic bacteria pathogenic for humans," *International Journal of Antimicrobial Agents*, vol. 36, no. 3, pp. 264–266, 2010, doi: 10.1016/j.ijantimicag.2010.04.008.
- [61] M. K. Kim *et al.*, "Antibacterial and antibiofilm activity and mode of action of magainin 2 against drug-resistant acinetobacter baumannii," *International Journal of Molecular Sciences*, vol. 19, no. 10, 2018, doi: 10.3390/ijms19103041.
- [62] Y. Park, D. G. Lee, and K. S. Hahm, "HP(2-9)-magainin 2(1-12), a synthetic hybrid peptide, exerts its antifungal effect on *Candida albicans* by damaging the plasma membrane," *Journal of Peptide Science*, vol. 10, no. 4, pp. 204–209, 2004, doi: 10.1002/psc.489.
- [63] J. Lehmann *et al.*, "Antitumor Activity of the Antimicrobial Peptide Magainin II against Bladder Cancer Cell Lines," *European Urology*, vol. 50, no. 1, pp. 141–147, 2006, doi: 10.1016/j.eururo.2005.12.043.
- [64] C. Wang, T. Hong, P. Cui, J. Wang, and J. Xia, "Antimicrobial peptides towards clinical application: Delivery and formulation," *Advanced Drug Delivery Reviews*, vol. 175, 2021, doi: 10.1016/j.addr.2021.05.028.
- [65] A. Rai *et al.*, "Antimicrobial peptide-based materials: opportunities and challenges," *Journal of Materials Chemistry B*, vol. 10, no. 14, pp. 2384–2429, 2022, doi: 10.1039/d1tb02617h.
- [66] B. A. Daniel Harris Lynn McNicoll, MD, Gary Epstein-Lubow, MD, and Kali S. Thomas, PhD, "Activity and characterization of a pH-sensitive antimicrobial peptide," *Physiology &*

- behavior*, vol. 1861, no. 10, pp. 139–148, 2019, doi: 10.1016/j.bbamem.2019.05.006.Activity.
- [67] Y. Nakajima, “Mode of Action and Resistance Mechanisms of Antimicrobial Macrolides,” *Macrolide Antibiotics: Chemistry, Biology, and Practice: Second Edition*, vol. 55, no. 1, pp. 453–499, 2003, doi: 10.1016/B978-012526451-8/50011-4.
- [68] J. Saraswat, F. A. Wani, K. I. Dar, M. M. A. Rizvi, and R. Patel, “Noncovalent Conjugates of Ionic Liquid with Antibacterial Peptide Melittin: An Efficient Combination against Bacterial Cells,” *ACS Omega*, vol. 5, no. 12, pp. 6376–6388, 2020, doi: 10.1021/acsomega.9b03777.
- [69] K. Ghaffar, W. Hussein, Z. Khalil, R. Capon, M. Skwarczynski, and I. Toth, “Levofloxacin and Indolicidin for Combination Antimicrobial Therapy,” *Current Drug Delivery*, vol. 12, no. 1, pp. 108–114, 2015, doi: 10.2174/1567201811666140910094050.
- [70] J. Shi, Y. Liu, Y. Wang, J. Zhang, S. Zhao, and G. Yang, “Biological and immunotoxicity evaluation of antimicrobial peptide-loaded coatings using a layer-by-layer process on titanium,” *Scientific Reports*, vol. 5, no. November, pp. 1–15, 2015, doi: 10.1038/srep16336.
- [71] F. Cao, L. Mei, G. Zhu, M. Song, and X. Zhang, “An injectable molecular hydrogel assembled by antimicrobial peptide PAF26 for antimicrobial application,” *RSC Advances*, vol. 9, no. 53, pp. 30803–30808, 2019, doi: 10.1039/c9ra06130d.
- [72] S. Baixe *et al.*, “Strongly adhesive and antimicrobial peptide-loaded, alginate–catechol-based gels for application against periimplantitis,” *Applied Sciences (Switzerland)*, vol. 11, no. 21, pp. 1–15, 2021, doi: 10.3390/app112110050.
- [73] M. Hartlieb, E. G. L. Williams, A. Kuroki, S. Perrier, and E. S. Katherine, “Original citation : Antimicrobial polymers : Mimicking amino acid functionality through to three-dimensional structure of host-defense peptides,” *Current Medicinal Chemistry*, vol. 24, 2017.
- [74] D. Vandamme, B. Landuyt, W. Luyten, and L. Schoofs, “A comprehensive summary of LL-37, the lactoferrin human cathelicidin peptide,” *Cellular Immunology*, vol. 280, no. 1, pp. 22–35, 2012, doi: 10.1016/j.cellimm.2012.11.009.
- [75] J. W. Larrick, M. Hirata, R. F. Balint, J. Lee, J. Zhong, and S. C. Wright, “Human CAP18: A novel antimicrobial lipopolysaccharide-binding protein,” *Infection and Immunity*, vol. 63, no. 4, pp. 1291–1297, 1995, doi: 10.1128/iai.63.4.1291-1297.1995.
- [76] C. C. Lee, Y. Sun, S. Qian, and H. W. Huang, “Transmembrane pores formed by human antimicrobial peptide LL-37,” *Biophysical Journal*, vol. 100, no. 7, pp. 1688–1696, 2011, doi: 10.1016/j.bpj.2011.02.018.

- [77] R. E. W. Hancock and H. G. Sahl, "Antimicrobial and host-defense peptides as new anti-infective therapeutic strategies," *Nature Biotechnology*, vol. 24, no. 12, pp. 1551–1557, 2006, doi: 10.1038/nbt1267.
- [78] A. G. Cairns-Smith, "4. Organisms," *The Life Puzzle*, vol. 415, no. January, pp. 51–64, 2017, doi: 10.3138/9781487589684-006.
- [79] J. Overhage, A. Campisano, M. Bains, E. C. W. Torfs, B. H. A. Rehm, and R. E. W. Hancock, "Human host defense peptide LL-37 prevents bacterial biofilm formation," *Infection and Immunity*, vol. 76, no. 9, pp. 4176–4182, 2008, doi: 10.1128/IAI.00318-08.
- [80] S. N. Dean, B. M. Bishop, and M. L. Van Hoek, "Susceptibility of *Pseudomonas aeruginosa* biofilm to alpha-helical peptides: D-enantiomer of LL-37," *Frontiers in Microbiology*, vol. 2, no. JULY, pp. 1–11, 2011, doi: 10.3389/fmicb.2011.00128.
- [81] M. Comune, A. Rai, P. Palma, C. Tondaturo, and L. Ferreira, "Antimicrobial and pro-angiogenic properties of soluble and nanoparticle-immobilized LL37 peptides," *Biomaterials Science*, vol. 9, no. 24, pp. 8153–8159, 2021, doi: 10.1039/d1bm01034d.
- [82] T. Dai, Y. Y. Huang, and M. R. Hamblin, "Photodynamic therapy for localized infections-State of the art," *Photodiagnosis and Photodynamic Therapy*, vol. 6, no. 3–4, pp. 170–188, 2009, doi: 10.1016/j.pdpdt.2009.10.008.
- [83] Y. Zou, Y. Zhang, Q. Yu, and H. Chen, "Photothermal bactericidal surfaces: Killing bacteria using light instead of biocides," *Biomaterials Science*, vol. 9, no. 1, pp. 10–22, 2021, doi: 10.1039/d0bm00617c.
- [84] Z. Qi *et al.*, "Multivalency at Interfaces: Supramolecular Carbohydrate-Functionalized Graphene Derivatives for Bacterial Capture, Release, and Disinfection," *Nano Letters*, vol. 15, no. 9, pp. 6051–6057, 2015, doi: 10.1021/acs.nanolett.5b02256.
- [85] J. W. Xu, K. Yao, and Z. K. Xu, "Nanomaterials with a photothermal effect for antibacterial activities: An overview," *Nanoscale*, vol. 11, no. 18, pp. 8680–8691, 2019, doi: 10.1039/c9nr01833f.
- [86] D. Hu *et al.*, "Surface-Adaptive Gold Nanoparticles with Effective Adherence and Enhanced Photothermal Ablation of Methicillin-Resistant *Staphylococcus aureus* Biofilm," *ACS Nano*, vol. 11, no. 9, pp. 9330–9339, 2017, doi: 10.1021/acsnano.7b04731.
- [87] Y. Zhu, M. Ramasamy, and D. K. Yi, "Antibacterial activity of ordered gold nanorod arrays," *ACS Applied Materials and Interfaces*, vol. 6, no. 17, pp. 15078–15085, 2014, doi:

10.1021/am503153v.

- [88] P. Pallavicini *et al.*, "Self-assembled monolayers of gold nanostars: A convenient tool for near-IR photothermal biofilm eradication," *Chemical Communications*, vol. 50, no. 16, pp. 1969–1971, 2014, doi: 10.1039/c3cc48667b.
- [89] S. Cabana *et al.*, "Silicone rubber films functionalized with poly(acrylic acid) nanobrushes for immobilization of gold nanoparticles and photothermal therapy," *Journal of Drug Delivery Science and Technology*, vol. 42, pp. 245–254, 2017, doi: 10.1016/j.jddst.2017.04.006.
- [90] O. Khantamat *et al.*, "Gold nanoshell-decorated silicone surfaces for the near-infrared (NIR) photothermal destruction of the pathogenic bacterium *E. faecalis*," *ACS Applied Materials and Interfaces*, vol. 7, no. 7, pp. 3981–3993, 2015, doi: 10.1021/am506516r.
- [91] L. Hui *et al.*, "Surface disinfection enabled by a layer-by-layer thin film of polyelectrolyte-stabilized reduced graphene oxide upon solar near-infrared irradiation," *ACS Applied Materials and Interfaces*, vol. 7, no. 19, pp. 10511–10517, 2015, doi: 10.1021/acsami.5b02008.
- [92] R. Kurapati, M. Vaidyanathan, and A. M. Raichur, "Synergistic photothermal antimicrobial therapy using graphene oxide/polymer composite layer-by-layer thin films," *RSC Advances*, vol. 6, no. 46, pp. 39852–39860, 2016, doi: 10.1039/c5ra23038a.
- [93] W. Lei *et al.*, "Polydopamine Nanocoating for Effective Photothermal Killing of Bacteria and Fungus upon Near-Infrared Irradiation," *Advanced Materials Interfaces*, vol. 3, no. 22, pp. 1–6, 2016, doi: 10.1002/admi.201600767.
- [94] S. H. Kim, E. B. Kang, C. J. Jeong, S. M. Sharker, I. In, and S. Y. Park, "Light Controllable Surface Coating for Effective Photothermal Killing of Bacteria," *ACS Applied Materials and Interfaces*, vol. 7, no. 28, pp. 15600–15606, 2015, doi: 10.1021/acsami.5b04321.
- [95] X. Teng *et al.*, "Rapid and highly effective bacteria-killing by polydopamine/IR780@MnO₂-Ti using near-infrared light," *Progress in Natural Science: Materials International*, vol. 30, no. 5, pp. 677–685, 2020, doi: 10.1016/j.pnsc.2020.06.003.
- [96] Y. Ren *et al.*, "Photoresponsive Materials for Antibacterial Applications," *Cell Reports Physical Science*, vol. 1, no. 11, p. 100245, 2020, doi: 10.1016/j.xcrp.2020.100245.
- [97] L. Hong *et al.*, "Rapid Biofilm Elimination on Bone Implants Using Near-Infrared-Activated Inorganic Semiconductor Heterostructures," *Advanced Healthcare Materials*, vol. 8, no. 19, pp. 1–11, 2019, doi: 10.1002/adhm.201900835.

- [98] Y. Yu, P. Li, C. Zhu, N. Ning, S. Zhang, and G. J. Vancso, "Multifunctional and Recyclable Photothermally Responsive Cryogels as Efficient Platforms for Wound Healing," *Advanced Functional Materials*, vol. 29, no. 35, pp. 1–11, 2019, doi: 10.1002/adfm.201904402.
- [99] Y. Ko *et al.*, "Antibacterial poly (3,4-ethylenedioxythiophene):poly(styrene-sulfonate)/agarose nanocomposite hydrogels with thermo-processability and self-healing," *Carbohydrate Polymers*, vol. 203, no. July 2018, pp. 26–34, 2019, doi: 10.1016/j.carbpol.2018.09.026.
- [100] L. I. of America, "American National Standard for Safe Use of Lasers," *Laser Institute of America*, 2007, [Online]. Available: papers2://publication/uuid/D2E145A0-6015-4317-895E-3644589A4A40.
- [101] X. Zhu *et al.*, "Temperature-feedback upconversion nanocomposite for accurate photothermal therapy at facile temperature," *Nature Communications*, vol. 7, pp. 1–10, 2016, doi: 10.1038/ncomms10437.
- [102] A. D'Agostino *et al.*, "Bulk surfaces coated with triangular silver nanoplates: Antibacterial action based on silver release and photo-thermal effect," *Nanomaterials*, vol. 7, no. 1, 2017, doi: 10.3390/nano7010007.
- [103] E. Faure *et al.*, "Catechols as versatile platforms in polymer chemistry," *Progress in Polymer Science*, vol. 38, no. 1, pp. 236–270, 2013, doi: 10.1016/j.progpolymsci.2012.06.004.
- [104] J. Yang, M. A. Cohen Stuart, and M. Kamperman, "Jack of all trades: Versatile catechol crosslinking mechanisms," *Chemical Society Reviews*, vol. 43, no. 24, pp. 8271–8298, 2014, doi: 10.1039/c4cs00185k.
- [105] X. Zhang *et al.*, "Endogenous 3,4-dihydroxyphenylalanine and dopaquinone modifications on protein tyrosine: Links to mitochondrially derived oxidative stress via hydroxyl radical," *Molecular and Cellular Proteomics*, vol. 9, no. 6, pp. 1199–1208, 2010, doi: 10.1074/mcp.M900321-MCP200.
- [106] C. C. Ho and S. J. Ding, "The pH-controlled nanoparticles size of polydopamine for anti-cancer drug delivery," *Journal of Materials Science: Materials in Medicine*, vol. 24, no. 10, pp. 2381–2390, 2013, doi: 10.1007/s10856-013-4994-2.
- [107] M. Ivarsson, M. Prekert, A. Cheema, P. Wretenberg, and N. Andjelkov, "Mussel Adhesive Protein as a Promising Alternative to Fibrin for Scaffold Fixation during Cartilage Repair Surgery," *Cartilage*, vol. 13, no. 2_suppl, pp. 663S-671S, 2021, doi:

10.1177/1947603519887319.

- [108] M. J. Harrington, F. Jehle, and T. Priemel, "Mussel Byssus Structure-Function and Fabrication as Inspiration for Biotechnological Production of Advanced Materials," *Biotechnology Journal*, vol. 13, no. 12, pp. 1–27, 2018, doi: 10.1002/biot.201800133.
- [109] J. Wang and T. Scheibel, "Recombinant Production of Mussel Byssus Inspired Proteins," *Biotechnology Journal*, vol. 13, no. 12, pp. 1–28, 2018, doi: 10.1002/biot.201800146.
- [110] R. M. Kosanke, "Mussel-Inspired Surface Chemistry for Multifunctional Coatings," *Science*, vol. 318, no. OCTOBER, pp. 426–431, 2019.
- [111] P. Salazar, M. Martin, and J. L. Gonzalez, "(PDF) Polydopamine-modified surfaces in biosensor applications," *Polymer science: research advances, practical applications and educational aspects*, vol. 1, no. July, pp. 385–396, 2016, [Online]. Available: https://www.researchgate.net/publication/305044131_Polydopamine-modified_surfaces_in_biosensor_applications.
- [112] L. Khalafi, M. Rafiee, M. Shahbak, and H. Shirmohammadi, "Kinetic study of the oxidation of catechols in the presence of N-methylaniline," *Journal of Chemistry*, vol. 2013, 2013, doi: 10.1155/2013/497515.
- [113] D. Nematollahi, E. Tammari, S. Sharifi, and M. Kazemi, "Mechanistic study of the oxidation of catechol in the presence of secondary amines by digital simulation of cyclic voltammograms," *Electrochimica Acta*, vol. 49, no. 4, pp. 591–595, 2004, doi: 10.1016/j.electacta.2003.09.013.
- [114] M. A. C. H. Ernard, K. A. K. Raehenbuehl, A. N. R. Ytz, and D. E. D. R. Oberts, "Interactions between Volatile and Nonvolatile Coffee Components. 1. Screening of Nonvolatile Components," 2005.
- [115] M. Nikolantonaki, M. Jourdes, K. Shinoda, P. Teissedre, and P. Darriet, "Identification of Adducts between an Odoriferous Volatile Thiol and Oxidized Grape Phenolic Compounds: Kinetic Study of Adduct Formation under Chemical and Enzymatic Oxidation Conditions," 2012.
- [116] S. H. Hong, S. Hong, M. H. Ryou, J. W. Choi, S. M. Kang, and H. Lee, "Sprayable Ultrafast Polydopamine Surface Modifications," *Advanced Materials Interfaces*, vol. 3, no. 11, pp. 1–6, 2016, doi: 10.1002/admi.201500857.
- [117] Z. Trzcińska, M. Bruggeman, H. Ijakipour, N. J. Hodges, J. Bowen, and A. Stamboulis, "Polydopamine linking substrate for AMPs: Characterisation and stability on Ti6Al4V,"

Materials, vol. 13, no. 17, pp. 1–19, 2020, doi: 10.3390/MA13173714.

- [118] A. Bourmaud, J. Riviere, A. Le Duigou, G. Raj, and C. Baley, “Investigations of the use of a mussel-inspired compatibilizer to improve the matrix-fiber adhesion of a biocomposite,” *Polymer Testing*, vol. 28, no. 6, pp. 668–672, 2009, doi: 10.1016/j.polymertesting.2009.04.006.
- [119] V. Ball, D. Del Frari, V. Toniazzo, and D. Ruch, “Kinetics of polydopamine film deposition as a function of pH and dopamine concentration: Insights in the polydopamine deposition mechanism,” *Journal of Colloid and Interface Science*, vol. 386, no. 1, pp. 366–372, 2012, doi: 10.1016/j.jcis.2012.07.030.
- [120] P. Zhou *et al.*, “Rapidly-deposited polydopamine coating via high temperature and vigorous stirring: Formation, characterization and biofunctional evaluation,” *PLoS ONE*, vol. 9, no. 11, pp. 0–9, 2014, doi: 10.1371/journal.pone.0113087.
- [121] S. Kasemset, A. Lee, D. J. Miller, B. D. Freeman, and M. M. Sharma, “Effect of polydopamine deposition conditions on fouling resistance, physical properties, and permeation properties of reverse osmosis membranes in oil/water separation,” *Journal of Membrane Science*, vol. 425–426, pp. 208–216, 2013, doi: 10.1016/j.memsci.2012.08.049.
- [122] J. Kang, S. Tada, T. Kitajima, T. Il Son, T. Aigaki, and Y. Ito, “Immobilization of bone morphogenetic protein on DOPA- or dopamine-treated titanium surfaces to enhance osseointegration,” *BioMed Research International*, vol. 2013, 2013, doi: 10.1155/2013/265980.
- [123] F. Bernsmann, V. Ball, A. Ponche, M. Michel, D. A. Gracio, and D. Ruch, “Bernsmann2011.Pdf,” pp. 2819–2825, 2011.